Geological Survey of Finland

Bulletin 326

Petrography, mineral chemistry and petrochemistry of granite porphyry dykes from Sibbo, southern Finland

by Ragnar Törnroos

Geologian tutkimuskeskus
Espoo 1984

Geological Survey of Finland, Bulletin 326

PETROGRAPHY, MINERAL CHEMISTRY AND PETROCHEMISTRY OF GRANITE PORPHYRY DYKES FROM SIBBO, SOUTHERN FINLAND

by

RAGNAR TÖRNROOS

with 22 figures and 13 tables

GEOLOGIAN TUTKIMUSKESKUS — GEOLOGISKA FORSKNINGSCENTRALEN
ESPOO — ESBO 1984

Törnroos, R., 1984. Petrography, mineral chemistry and petrochemistry of granite porphyry dykes from Sibbo, southern Finland. *Geological Survey of Finland, Bulletin 326.* 43 pages, 22 figures and 13 tables.

Proterozoic porphyry dykes (1633 Ma) in Sibbo form a roughly 13-km-broad swarm oriented northwest, starting from the Onas granite and extending about 20 km to the NW. Petrochemical, mineral chemical and X-ray data are given for the majority of the 25 dykes encountered.

The porphyry dykes are of granitic composition with only small differences in mineralogy and texture. Petrochemical and mineral chemical data are given and discussed. Most of the plagioclase phenocrysts are zoned and occur in the range An_{70} - An_0. The groundmass plagioclase has the same composition, except that albite is more abundant. X-ray diffraction studies show that the K-felspar, both phenocrysts and in the groundmass, range from orthoclase to maximum microcline. Iron-rich biotite is the most abundant mafic mineral. Hastingsite, ferropargasite and ferroedenitic hornblende occur in almost all dykes, except of some very acid ones. Orthoferrosilite, pigeonite and fayalite are sparesly encounted only in two dykes. Petrochemically the dykes are closely related to the Onas granite, a small stock of rapakivitic composition. The dykes exhibit a slight differentiation: SiO_2 ranging from 59 wt % to 73 wt %, and ending in the composition of the Onas granite.

It is proposed that the dykes were emplaced in extension cracks generated by compression of the bedrock during the Middle Proterozoic orogeny (1800 Ma) and regenerated as en echelon fractures by rapakivi magmatism in southern Finland and especially by the intrusion of the small Onas granite (1630 Ma) in the late Middle Proterozoic.

Key words: Granite porphyry dykes, petrography, petrochemistry, mineral chemistry, Sibbo, Sipoo, Finland.

Ragnar Törnroos,
Geological Survey of Finland
Stenkarlsvägen 1, SF-02150 Esbo 15, Finland

ISBN 951-690-200-6
ISSN 0367-522X

CONTENTS

408400497K

INTRODUCTION

Twenty-five granite porphyry dykes trending roughly NW-SE constitute a dyke swarm in southern Sibbo, 20—30 km east of Helsingfors (Helsinki in Finnish) (Fig. 1). Some of the dykes have already been described and discussed by Borgström (1907, 1947) and Saastamoinen (1956). Several new dykes have been observed during mapping activities in the area (Härme 1978), and in the summer of 1982 the present author reinvestigated the dykes. Fresh road and railway cuttings have revealed new localities, some of which are very informative.

All 21 numbered dykes in Fig. 1 have been studied by microscope and the majority also by electron probe instrument (EPI), X-ray diffraction and XRF whole-rock analyses. The intention of this study is to throw fresh light on the genesis of the dykes using the above methods.

GEOLOGICAL OUTLINE

The dyke swarm at Sibbo cuts the Proterozoic (1800 Ma) Svecofennidic gneisses, migmatites and granites of the area. The distribution of the Sibbo dykes is shown in Fig. 1. With some exceptions, the direction of the dykes is NW-SE. The dip is mostly vertical. The dykes crop out at several places along lines trending NW-SE, roughly constituting three dyke systems referred to here as A, B and C.

Dyke system A begins at Fårholmen (No. 107) near the Skyttenskär archipelago and may be followed for about 17 km through Östersundom to dyke No. 3 in Vanda. Dyke system B (Nos. 50 and 51) is rather short, but the fissure has been intruded twice, giving rise to a composite dyke: the NW part consists of a diabase breccia and the SE part is granite porphyry. Dyke system C may be followed for at least 20 km from Spjutsund to Vallkulla (No. 31, ca 3 km SW of the church of Sibbo (Nickby)). Nos. 28 and 40 can be observed in road and railway cuttings on the Nickby—Sköldvik road.

Some of the dykes crop out for up to 2 km, but normally for only a few metres or tens of metres. From aerial photographs the dykes may be traced as low channel-like lineaments. Being covered with soil and vegetation they are usually difficult to detect in exposed rock. In some places the width of the dykes changes gradually; in others rather abruptly. In a few places the dykes split up into several parallel veins (Fig. 2). The width of the dykes is normally 3—5 m, but may vary from some cm to 10 m.

Borgström (1947) points out that the fissure into which the granite porphyry magma intruded was not a continuous open crack of uniform breadth and was closed along part of its length.

The dykes commonly show internal fracturing. In places a three system fracturing with angles of about 120° forms six-sided prisms that resemble the pillars of basalts. These cracks never cross the boundary of the dykes. Other cracks, however, may continue from the dyke into the country rock.

The dykes are genetically closely related to the small Onas rapakivi granite. All the dykes described in this work are on the western side

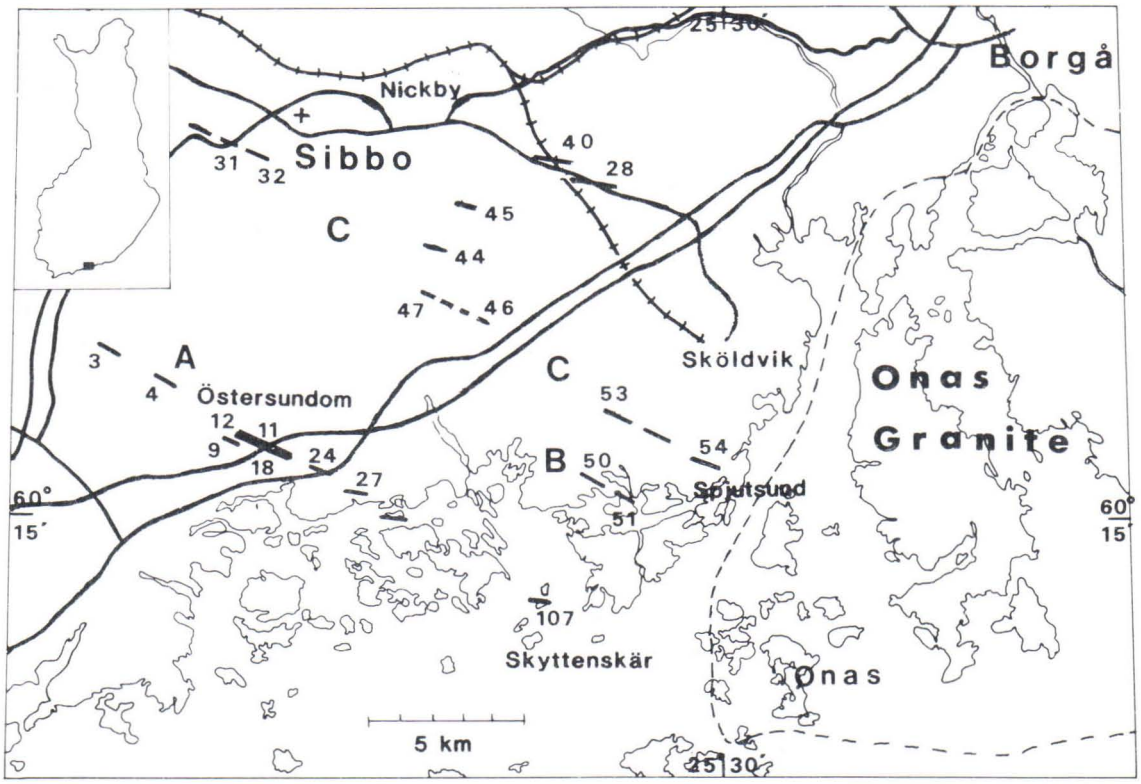

Fig. 1. Map showing the location of the Sibbo dykes. Dyke A begins at Fårholmen (No. 107) near the Skyttenskär archipelago and ends at No. 3 near the N-S trending shear zone indicated by the two highways in the left side of the map. Dyke B constitutes a composite dyke on Silverlandet, where No. 50 is a diabase breccia and No. 51 a porphyry dyke. Dyke C begins at Spjutsund with No. 54 and ends with No. 31 near the village of Sibbo. There are also several separate dykes in the area.

of the Onas granite. On the eastern side only one granite porphyry dyke has been encounered so far, on an islet south of Julö a small island in the Pellinge archipelago, parish of Borgå (Laitala 1984) (not shown on map, Fig. 1). This is the second composite dyke known to the author the area around the Onas granite. The fissure first intruded by a diabase magma. Later, during the rapakivi intrusion, the central part of the dyke was occupied by granite porphyry (Laitala 1984, Fig. 20, p. 39).

PETROGRAPHY

Good microscopical descriptions of the granite porphyry of Sibbo have been given by Borgström (1907, 1947) (southeastern part of dyke A, Nos. 107—12, Fårholmen—Östersundom) and Saastamoinen (1956) (dyke B and the southeastern part of dyke C, Nos. 54—47, Spjutsund—Tasträsk).

The granite porphyry is a fine-grained rock

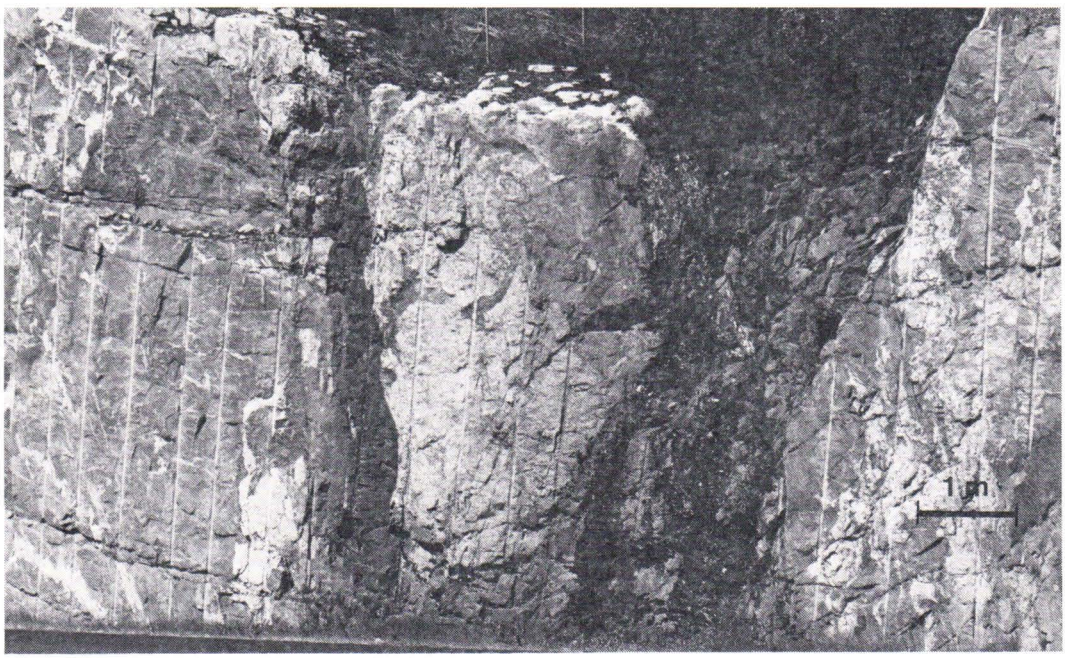

Fig. 2. Forking of dyke No. 11. Roadcutting at Östersundom.

(aphanitic to 0.3 mm) with aphanitic contacts. It is dark brown except on weathered surfaces, where it is reddish. The texture is porphyritic with phenocrysts making up 5—10 vol % of the rock. The main constituents are K-felspar (in places up to 2 cm long), quartz, plagioclase (An_0 - An_{70}) with smaller amounts of biotite, hornblende, apatite, fluorite and magnetite-ilmenite. The quartz and plagioclase phenocrysts are normally smaller than the K-felspar ones, *i.e.* from ca. 2 mm down to microphenocrystic in size. The numbers of phenocrysts varies greatly; in a normal thin section there may be from one to about a dozen. Near the contacts the phenocrysts generally become smaller and more numerous, and in some dyke rocks they consist mostly of plagioclase, as in the dykes at Vallkulla (Nos. 31 and 32) where there are abundant plagioclase and magnetite-ilmenite phenocrysts in an orb-like spherulitic groundmass.

Quartz, which makes up 30—40 vol % of the phenocrysts, occurs as euhedral to subhedral hexagonal bipyramides. Because of magmatic resorption, the quartz phenocrysts are more or less rounded and corroded, in places considerably so. Undulatory extinction is rare. The quartz crystals are nearly free of inclusions but normally have an outer narrow reaction rim with groundmass inclusions. Some quartz grains exhibit rows of fluid inclusions following earlier cracks in the grains. The fluid bubbles disappear when exposed to strong light under the microscope (without polariser) and reappear when the light intensity is reduced again. This indicates liquid CO_2 that disappears as a CO_2 mist at a temperature of 28°—32° C (see *e.g.* Roedder 1972).

Plagioclase (10—15 vol % of the phenocrysts) is colourless, mostly rectangular and euhedral. Sometimes it is corroded and in places almost totally replaced by hornblende, muscovite, calcite and fluorite.

K-felspar constitutes the bulk of the phenocrysts (50—60 vol %). They are euhedral, in places with slightly rounded corners. Micro-

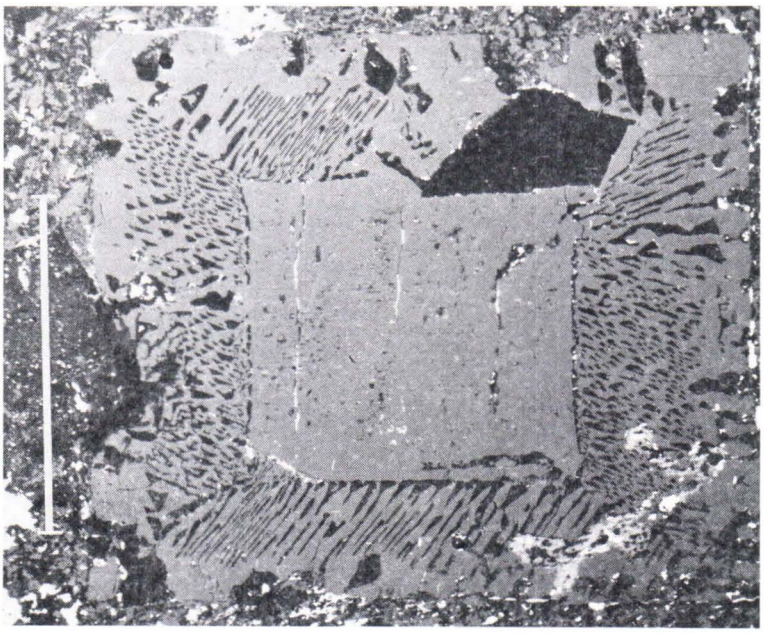

Fig. 3. Backscattered electron image of a K-felspar phenocryst with a zone (zones) of intergrown quartz. Dyke No. 44, Stor Annas sten. Polished thin section, length of bar 1.0 cm.

cline is most common, but orthoclase also occurs.

The most striking feature of the rock sections under the microscope is the spectacular graphic texture of the K-felspar phenocrysts (Figs. 3, 4, 5). The quartz inclusions occur as rounded or vermicular grains in the K-felspars, either as beautiful zones (Fig. 3) or filling the whole or only the centre of the phenocryst (Fig. 4). The quartz inclusions have uniform optical orientation in large portions or over the whole of the phenocryst. Thorough examination of the thin sections revealed that around the quartz inclusions there are some corroded portions filled with groundmass material, in places also calcite, fluorite and native metal (Figs. 5 and 21).

Borgström (1907) attributed these granophyric textures to eutectic crystallisation of quartz and felspar. Other processes as well, however, may also produce granophyric textures; some of those proposed are devitrification, exsolution, metasomatism, vapour deposition, coupled and noncoupled growth, and magmatic crystallisation (*e.g.* Drescher-Kaden 1948, 1969, 1974; Barker 1970; Augustithis 1973; Smith 1974; Carstens 1983). These various possibilities have been discussed in detail by Smith (*op.cit.*) and Carstens (*op.cit.*).

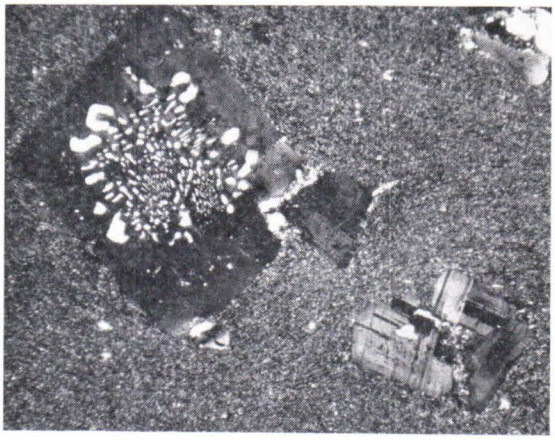

Fig. 4. Photomicrograph showing K-felspar and plagioclase phenocrysts with intergrown quartz filling up the the centre of the crystals. Polished thin section, crossed polarisers, 10 X.

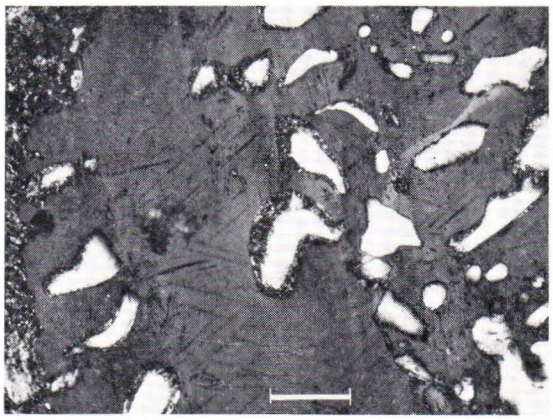

Fig. 5. Photomicrograph of a K-felspar phenocryst with intergrown quartz. Around the quartz grains are corroded zones filled with groundmass material and secondary minerals (cf. Fig. 21). The lamellar structure is composed of a very An-rich plagioclase, length of bar 100 μm.

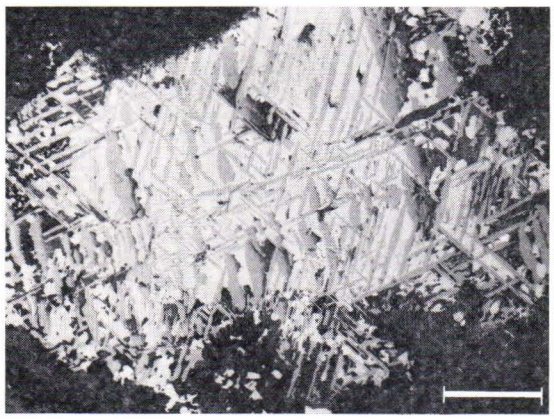

Fig. 6. Compositional backscattered electron image (BEI Compo) of a ilmenomagnetite phenocryst. Grey ilmenite lamellae constitute a network pattern in the magnetite. The halo around the phenocryst consists of titanite (dark grey) and amphibole + some biotite (black). Polished thin section, dyke No. 31, length of bar 100 μm.

New aspects of the genesis of alkali felspar phenocrysts have been introduced in recent investigations by Winkler and Schultes (1982). According to them, alkali felspar phenocrysts may precipitate at each stage of magmatic crystallisation, provided that the amount of liquid (melt) exceeds 30—40 %. They also pointed out that 65—70 % of the total system was still liquid when the cotectic crystallisation of plagioclase, quartz and alkali felspar began. The temperature was then only 6°—11°C above the solidus temperature for the granites investigated.

Mehnert and Büsch (1981) have studied the distribution of the Ba content in alkali felspar phenocrysts in granites, quartz porphyries and granite porphyries from the Schwarzwald. They conclude that the phenocrysts of the granites consist of two or more cores of old K-felspar, which probably floated in a still liquid environment (magma) of relatively low viscosity. The small crystals, then forced to grow together, were incorporated in and adopted the crystal structure of the growing megacryst. On the other hand, the Ba distribution shows that the phenocrysts in the porhyries have only one core. Hence Mehnert and Büsch (*op.cit.*) suggest that the cores of the phenocrysts are formed during a relatively quiet, undisturbed "intertelluric" phase of crystallisation that is followed by a stage of greater disturbance: the formation of the shells of the phenocrysts.

Magnetite and ilmenomagnetite occur as small phenocrysts from 0.5 to 1 mm in size. The ilmenite appears as an exsolution network in titanomagnetite (Fig. 6), with secondary titanite as a reaction product. In some grains the ilmenite has a skeleton structure in which the interspaces are filled with calcite, biotite and sparse titanite. Small grains of apatite and Ti-rich biotite also occur within the phenocrysts.

Sparse euhedral magnetite phenocrysts that are sometimes corroded and contain inclusions of alkali felspar were encountered in some of the dyke rocks.

All these oxide phenocrysts are surrounded by halos of biotite and hornblende somewhat coarser than in the groundmass.

The major constituents of the groundmass are felspar, quartz, biotite and hornblende. The minor constituents are apatite, calcite,

Table 1. Pointcounter analyses of some granite porphyry dykes from Sibbo (vol %).

	1	2	3	4	5	6	7
K-felspar	48.5		37.8	31.6	32.8	32.5	34.2
Quartz	28		16.1	11.7	21.4	11.0	12.6
Plagioclase	11.8		7.4	9.5	8.5	4.9	4.5
Biotite	10.5		18.8	12.1	22.9	27.4	20.9
Hornblende			13.9	9.2	5.9	11.9	7.6
Calcite			0.4	0.5	0.6	0.4	1.9
Fluorite		1.5	0.1	0.6	0.9		
Apatite			0.4		0.1	0.2	
Zircon				0.2		0.1	
Ilmenite + magnetite			0.3	2.0	0.4	0.6	1.1
Accessories	1.2						
Granophyre			4.8	22.6	6.5	11.0	12.2
Total	100.0		100.0	100.0	100.0	100.0	100.0

1) Granite porphyry from Spjutsund (Saastamoinen 1956)
2) Fluorite determination on one especially fluorite-rich thin section of the dyke at Spjutsund (Saastamoinen 1956)
3) Granite porphyry No. 3C, Bisaträsk, Vanda
4) ,, No. 11A, Östersundom
5) ,, No. 31A, Vallkulla, Sibbo Kyrkoby
6) ,, No. 40A, The road and railway cutting on the Nickby—Sköldvik road, parish of Borgå
7) ,, No. 45A, Nynäs

fluorite, pyroxene, zircon and secondary chlorite. Near the contacts the groundmass consists almost entirely of spherulites interspersed with some quartz, felspar and hornblende.

Table 1 gives pointcounter analyses of the more coarse-grained central parts of some of the dykes. Plagioclase and K-felspar are difficult to distinguish and errors may arise in the K-felspar—plagioclase ratio. If the values in Table 1 are compared with the CIPW norms in Tables 2 and 3 it is obvious that the plagioclase has been underrated in the pointcounter analyses. Nearer the contacts the plagioclase content seems to increase.

Biotite and hornblende occur as randomly oriented platy grains 0.1 mm in size in the central parts of the dykes; nearer the contacts they become smaller and elongated, imparting a clear flow structure to the rock. The biotite has strong pleochroism, α and β dark brownish green, γ pale yellow green, and is sometimes very much like hornblende. The microprobe analyses of biotite and hornblende are given in Tables 9 and 10. The green spots sometimes seen in thin section were revealed under the microscope to be accumulations of biotite and hornblende. Borgström (1907) assumed that they were pseudomorphs after pyroxene, an assumption that is supported by the presence of very sparse grains of relict orthopyroxene (orthoferrosilite) (analysis in Table 10).

The K-felspar is shown by X-ray to be microcline (Fig. 18, p. 28). In the central parts of the thicker dykes the felspar frequently develops beautiful granophyric intergrowths with quartz. Borgström (1907, 1947) has described five modes of such intergrowths: rhopalophyric, radiating fringe and cuneiform according to the nomenclature of Riederer (1965) and Barker (1970), and also plumose and vermicular. Microprobe analyses (beam diam. = 50 μm) of such granophyric intergrowths reveal that they have a clacium component, too (Table 3, point 12). Comparison with the analyses of the dyke rocks shows that the granophyres resemble the dykes in composition. Only SiO_2 and FeO differ, indicating

the more acid nature of the granophyric parts as a result of the lack of biotite and hornblende.

Fluorite occur sparsely in some places and more abundantly in others both in small cavities and as anhedral grains in the groundmass. It also replaces plagioclase together with muscovite and calcite. It varies from colourless to violet. Using the pointcounter method Saastamoinen (1956) has estimated that the dyke rock at Spjutsund has 1.5 % fluorite, some of which seems to be primary.

Apatite and zircon occur as rare small subhedral prisms. Here and there calcite fills cavities together with quartz and fluorite and also occurs as a replacement product after plagioclase and ilmenite. It is often seen in the tails of the phenocrysts.

Spherulites become frequent nearer the contacts, and in places they build up an orb-like structure. The radiating structure of the spherulites seems to be poorly developed in the backscattered electron image (BEI) (Fig. 7), being more like a granophyre with randomly scattered very small laths and spots of amphibole, biotite and magnetite-ilmenite. This is because the BEI reveals only the "compositional" condition right on the surface, whereas the optical microscope allowes one to "look under the surface". Between crossed nicols the spherulites show sharp interference crosses such as described by Rosenbusch-Osann (1923). These crosses, which are consistent with a radiating structure, have also been described by Borgström (1907) and Saastamoinen (1956) from the Sibbo dyke rocks.

The bulk composition of the spherulites was determined by microprobe (beam diam. = 50 μm). The result is given in Table 3, column 10. The BE image in Fig. 7 shows that the spherulites are extremely fine grained with an interspace of a somewhat more coarse-grained mass. Qualitative interpretation with the microprobe shows that the dark parts are quartz and the light grey parts K-felspar. The white laths are biotite and amphibole or K-rich amphibole or even an intergrowth of biotite and amphibole. The rounded spots are partly magnetite and magnetite-ilmenite and partly amphibole and biotite. Line scanning profiles through the spherulite illustrate their complex structure with K-felspar, albite, plagioclase and quartz (Fig. 7). The spherulites are therefore

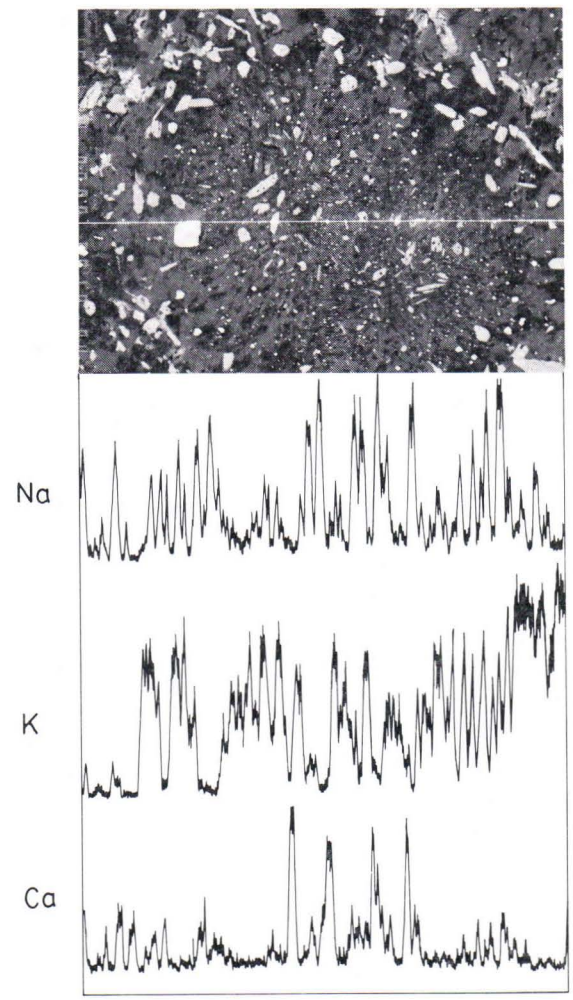

Fig. 7. BEI (compo) of spherulites near contact in dyke No. 11 and line scanning profiles of Na, K, and Ca (white line). The white parts are minerals with heavier elements, in this case amphibole and biotite. Grey is alkali-felspar and black quartz. The more coars-grained interspherulitic mass (seen around the spherulite) contains more amphibole and biotite. Polished thin section, length of bar 10 μm.

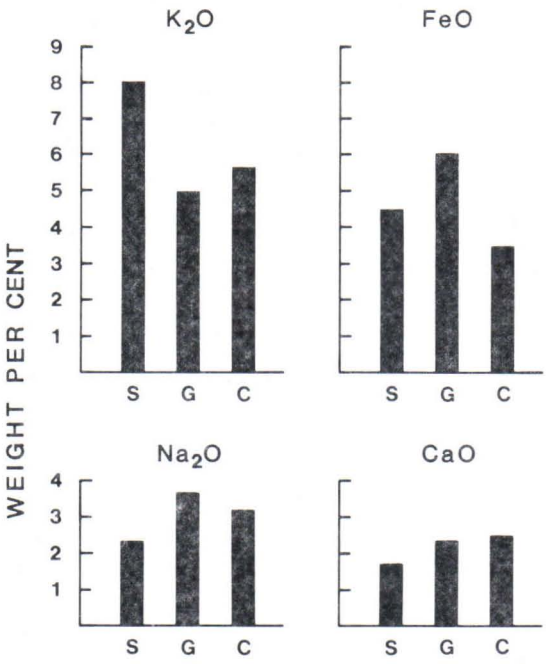

Fig. 8. Histograms showing the partition of K, Fe, Na and Ca between spherulite (S), groundmass of the dyke (G) and the narrow contact zone of the dyke (C). The spherulites are clearly enriched in K and depleted in the others when iron is enriched in the groundmass.

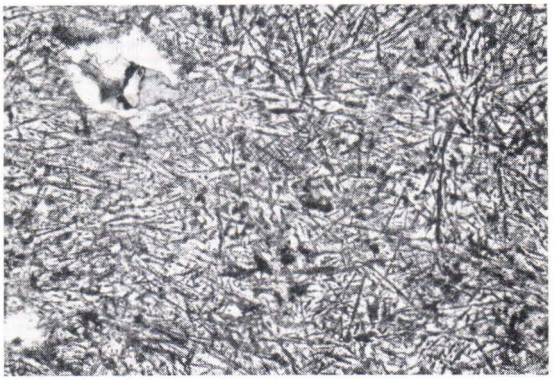

Fig. 9. Photomicrograph showing black needles of amphibole and biotite crystallites together with two amygdales filled with quartz, chlorite and biotite. Dyke No. 18, polished thin section, plane polarised light, 80 X.

composed of alkali felspar and quartz with some less calcic plagioclase. The more corse-grained interspherulitic mass contains more amphibole and biotite. This is also seen in the iron contents: Fe = 4 wt % in the spherulites and 8 wt % in the interspherulitic mass. An interesting zonal pattern is revealed by the Ca distribution. The black central part of the spherulite consists of plagioclase (Ca + Na). Then calcium is uniformly distributed (with the exception of some amphibole), whereas K-felspar and Na-felspar occur together with intergrown quartz, constituting a crude radial structure.

The compositions of the spherulites, the groundmass and the very narrow contact zone of the dyke rocks (compared in Fig. 8) were obtained by microprobe. The results of these analyses indicate that potassium prefers the spherulites whereas sodium, calcium and iron are enriched in the groundmass.

An especially odd structure is seen in the rocks of dykes 11 (a small branch) and 18. Over 50 % of the groundmass consists of needle-like crystallites and microliths (Fig. 9) with length-slow optical properties. In some instances they have been identified as hornblende and biotite by microprobe. The remainder are very fine-grained and consist, as determined by X-ray, mostly of quartz and K-felspar. Phenocrysts of pyroxene and olivine have also been encountered in these dyke rocks. Table 2 gives the results of an XRF analysis the rock of dyke No. 18. This rock is somewhat more basic than the other dyke rocks analysed.

Amygdales are common and are filled with secondary quartz, biotite, calcite, magnetite, fluorite and chlorite.

The extremely fine grain size of the groundmass together with the crystallites and microliths imply that some of the dyke rocks probably have a glassy origin.

PETROCHEMISTRY

Volcanic rocks have been classified on the basis of their chemical composition and the parameters derived from it by many investigators (*e.g.* Nockolds 1954; Irvine & Baragar 1971; Middlemost 1972; Le Maitre 1976; Streckeisen & Le Maitre 1979; de La Roche *et al.* 1980). In the present study the classification is based mainly on that by Irvine and Baragar (1971) and Streckeisen and Le Maitre (1979). Tables 2 and 3 list representative chemical compositions, Niggli values and the CIPW norms of the Sibbo dyke rocks and of the Onas granite.

Analytical techniques

Analyses 2—3 and 7 in Table 2 were done by wet chemical techniques and have been published before; the remainder are new XRF analyses done by Mr. V. Hoffrén. The lanthanoide analyses (Table 6) of samples 1, 8 and 9 were performed by Miss M. Kaistila by means of neutron activation. All the other analyses were done by the author using a JEOL JCXA-733 electron microprobe. The results of the rock analyses are listed in Tables 2 and 3. The whole rock microprobe analyses were performed using a defocused electron beam 50 μm in diameter. The microprobe was programmed to collect the intensities from four points in a square pattern with a step interval of 55 μm. The analyses were then calculated with a standard ZAF-on line reduction procedure using the mean intensities for each element from the four points. The areas selected for the analyses were without phenocrysts. This analytical method is admittedly crude, but because the dyke rocks are very fine grained, especially near the contacts, it does provide a quick way of obtaining satisfactory results.

Routine working techniques were used for the rest of the microprobe analyses. The accelerating voltage was set at 15 kV and the probe current at 15 nA. The standards used were natural minerals: anorthoclase for Si, Al and Na, garnet for Fe, biotite for Ti, Mg and K, celestine for Sr and Ba, and apatite for Ca (and P when analysed). The X-ray lines used were L_α for Ba and Sr, and K_α for the others.

The Ba line profiles (Figs. 16 and 17) were scanned by programming the instrument to move the specimen under the electron beam at a rate of 1 μm/s.

Major elements

The SiO_2 content ranges from 59.2 to 72.8 wt % in the analysed specimens. The rocks are quartz normative and plot in the subalkaline field (Fig. 10) of the alkali—silica diagram by Irvine and Baragar (1971). Some dyke rocks contain normative corundum but most contain diopside. The shift from diopside to corundum normative is gradual.

Almost all the Sibbo dyke rocks described plot in the rhyolite area (fields 2—3a) of the Q'- ANOR diagram of Streckeisen and Le Maitre (1979). The Onas granite also plots in the same area (granite) (see Fig. 11). The most basic rock, dyke No. 40, falls in field 3b.

The Niggli values for the dyke rocks and the Onas granite have been plotted in a *si-al, si-fm,*

Table 2. Selected analyses of the Onas granite and the dykes from Sibbo (wt. %). (XRF analyses by Mr. Väinö Hoffrén, Geological Survey of Finland).

	1	2	3	4	5	6	7	8	9
SiO_2	70.78	71.08	73.78	59.23	62.68	64.67	66.73	67.10	69.11
TiO_2	0.31	0.29	0.24	1.10	0.70	0.71	0.69	0.72	0.43
Al_2O_3	14.00	14.26	11.52	12.60	12.59	11.96	15.27	12.80	13.29
Fe_2O_3	3.83*	1.12	1.35	12.35*	10.56*	7.96*	1.47	7.36*	6.81*
FeO	—	2.31	2.37	—	—	—	3.41	—	—
MnO	0.07	tr	0.06	0.15	0.13	0.12	0.07	0.11	0.08
MgO	0.57	0.53	tr	0.54	0.34	0.39	0.44	0.49	0.55
CaO	1.08	0.96	0.92	3.26	2.71	2.16	2.94	2.44	1.54
Na_2O	3.59	3.49	2.50	2.08	2.27	2.34	2.79	3.06	3.13
K_2O	6.35	5.61	6.49	5.45	5.92	6.12	5.30	6.08	6.06
P_2O_5	0	tr	0.05	0.34	0.14	0.14	0.12	0.12	0.05
CO_2	nd	nd	nd	0.4	0.4	0.7	nd	nd	nd
H_2O_{tot}	nd	0.60	0.66	1.00	0.82	0.76	1.08	nd	nd
Total	100.38	100.25	99.94	98.50	99.24	98.02	100.31	100.28	101.03
Ba	0.19		0.13	0.09	0.06	0.23		0.21	0.01
Rb	0.012			0.021	0.022	0.030		0.014	0.026
Zr	0.041		0.07	0.080	0.098	0.074		0.082	0.076
				Niggli values					
si	341.46	356.15	424.36	222.37	252.10	291.21	291.31	287.20	308.62
al	39.80	42.10	39.05	27.88	29.84	31.74	39.28	32.28	34.97
fm	18.29	17.86	17.53	38.39	34.44	30.05	20.40	27.23	26.85
c	5.58	5.15	5.67	13.11	11.68	10.42	13.75	11.19	7.37
alk	36.33	34.88	37.75	20.62	24.04	27.79	26.56	29.30	30.81
mg	0.22	0.22	0	0.08	0.06	0.09	0.14	0.11	0.14
k	0.54	0.51	0.63	0.63	0.63	0.63	0.55	0.57	0.56
ti	1.12	1.09	1.04	3.11	2.12	2.40	2.26	2.32	1.44
p	0	0	0.12	0.54	0.24	0.28	0.22	0.22	0.10
h		10.03	12.66	12.52	11.00	11.41	15.73		
				CIPW norms					
Q	22.87	25.17	31.92	21.07	22.71	25.02	21.83	22.16	24.38
C	0	0.70	0	0	0	0	0	0	0
or	37.52	33.15	38.35	32.20	34.98	36.16	31.32	35.93	35.81
ab	30.38	29.53	21.15	17.60	19.21	19.80	23.61	25.89	26.49
an	3.33	4.76	1.04	8.95	6.68	4.06	13.49	3.23	4.32
di	0.95	0	2.85	0	1.09	0	0.27	2.63	1.41
wo	0	0	0	0	0	0	0	1.10	0
hy	0	4.16	1.44	1.35	0.34	0.97	5.00	0	0.72
mt	0	1.62	1.96	0	0	0	2.13	0	0
hm	3.83	0	0	12.35	10.56	7.96	0	7.36	6.81
il	0.15	0.55	0.46	0.32	0.28	0.26	1.31	0.23	0.17
ti	0.57	0	0	1.74	1.36	0.93	0	1.46	0.83
ap	0	0	0.12	0.81	0.33	0.33	0.28	0.28	0.12
ru	0	0	0	0.22	0	0.20	0	0	0
ca	0	0	0	0.91	0.91	1.59	0	0	0
Plag (An)	10	14	5	34	26	17	36	11	14
DI	90.77	87.85	91.42	70.87	76.90	80.98	76.76	83.98	86.68

* Total iron, nd = not determined, tr = traces

1) Onas granite, (XRF) (x = 6691,15 y = 422,41)
2) Onas granite, (Hackman 1905), wet chemical anal.
3) Onas granite, (Borgström 1931), wet chemical anal.
4) Granite porphyry No. 40, A road and railway cutting on the Nickby—Sköldvik road, parish of Borgå, (XRF), (x = 6694,80 y = 577,40)
5) ,, No. 31, Vallkulla, Sibbo Kyrkoby, (XRF), (x = 6694,85 y = 567,18)
6) ,, No. 18, Östersundom, (XRF), (x = 6685,50 y = 567,88)
7) ,, Östersundom, (Borgström 1907), wet chemical anal.
8) ,, No. 11, Östersundom, (XRF), (x = 6685,10 y = 568,20)
9) ,, No. 54, Spjutsund, (XRF), (x = 6684,73 y = 582,35)

Table 3. Selected microprobe analyses of the Sibbo dyke rocks (wt. %).

	1	2	3	4	5	6	7	8	9	10	11	12
SIO_2	66.32	66.74	67.43	67.65	69.83	69.90	72.73	72.77	69.60	69.86	69.04	75.80
TiO_2	0.95	0.74	nd	0.59	0.36	0.21	0.69	0.04	0.52	0.38	0.45	0.17
Al_2O_3	12.81	12.73	12.60	12.71	12.91	15.13	11.99	11.74	12.78	12.52	12.98	12.98
FeO*	8.17	6.38	6.34	6.68	6.06	1.79	5.16	2.67	2.42	4.50	3.48	0.50
MnO	0.07	0.07	nd	0.09	0.10	0.04	0	0.02	0.11	0.07	0.07	0.06
MgO	0.39	0.08	nd	0.19	0.19	0.17	0.22	0.02	0.03	0.11	0.33	0.02
CaO	2.05	2.32	2.27	2.95	2.36	0.09	1.86	0.72	1.78	1.71	2.47	1.43
Na_2O	3.30	4.15	3.20	2.42	3.63	1.53	3.77	4.88	1.92	2.31	3.18	3.13
K_2O	6.38	6.31	5.94	6.65	4.96	10.68	4.67	3.42	9.58	8.02	5.63	3.99
P_2O5	0.13	0.23	nd	0.20	0.24	0.04	0.21	0.08	nd	nd	0.10	0.05
Total	100.57	99.75	97.78	100.13	100.64	99.56	101.30	96.43	98.74	99.48	97.73	98.13
Ba					0.08		0.41					0.22
					Niggli values							
si	270.84	283.40	305.80	291.79	313.77	366.12	357.66	431.06	355.62	339.93	337.92	496.75
al	30.23	31.85	33.67	32.31	34.18	46.70	34.75	40.98	38.48	35.90	37.44	50.13
fm	30.52	23.41	24.05	25.65	24.43	9.34	22.83	13.50	11.05	19.40	16.94	3.27
c	8.97	10.55	11.03	13.63	11.36	0.51	9.80	4.57	9.74	8.92	12.95	10.04
alk	29.68	34.17	31.25	28.41	30.03	43.45	32.62	40.94	40.73	35.79	32.66	36.56
mg	0.08	0.02		0.05	0.05	0.14	0.07	0.01	0.02	0.04	0.14	0.06
k	0.56	0.50	0.55	0.64	0.47	0.82	0.45	0.32	0.77	0.70	0.54	0.46
ti	2.92	2.36		1.91	1.22	0.83	2.55	0.18	2.00	1.39	1.66	0.84
p	0.22	0.41		0.36	0.46	0.09	0.44	0.20			0.21	0.14
					CIPW norms							
Q	13.66	14.06	17.82	18.84	21.45	18.42	26.68	28.38	20.30	20.18	22.39	39.03
C	0	0	0	0	0	0.99	0	0	0	0	0	1.03
or	37.70	37.29	35.10	39.30	29.31	63.11	27.60	20.21	56.61	47.39	33.27	23.58
ab	27.92	30.45	27.08	20.48	30.72	12.95	31.90	41.29	12.40	19.55	26.91	26.49
an	1.30	0	2.47	4.18	4.28	0.19	2.00	0.03	0	0.11	4.52	6.77
di	7.08	8.90	7.84	8.11	5.19	0	5.17	2.69	7.29	7.43	6.19	0
wo	0	0	0	0	0	0	0	0	0.26	0	0	0
hy	10.81	6.10	7.48	7.65	8.45	3.44	6.16	3.50	0	4.11	3.37	0.80
il	1.80	1.41	1.12	0.68	0.40	1.31	0.08	0.99	0.72	0.86	0.32	
ap	0.31	0.55	0.47	0.57	0.10	0.50	0.19	0.24	0.12			
Plag (An)	4	0	8	17	12	1	6	0	0	1	14	20
DI	79.28	81.80	80.00	78.62	81.48	94.48	86.18	89.88	89.31	87.12	82.57	89.10

* Total iron, tr = traces, nd = not determined

1) Granite porphyry No. 28, A road cutting, Lövkulla, parish of Borgå, (x = 6694,12 y = 578,57)
2) ,, No. 32, near contact, Vallkulla, Sibbo Kyrkoby, (x = 6694,79 y = 567,54)
3) ,, No. 11, Östersundom.
4) ,, No. 9, Ringberga, Östersundom, (x = 6685,20 y = 566,92)
5) ,, No. 11, Östersundom.
6) ,, No. 51, Träskby,Silverlandet, (x = 6683,64 y = 579,87)
7) ,, No. 107, Fårholmen, (x = 6680,30 y = 577,20)
8) ,, No. 47, Tasträsk, (x = 6690,10 y = 574,06)
9) Border of the green spherulite (anal. No. 10).
10) Spherulite (green) in dyke 11, Östersundom.
11) Contact of dyke 11, Östersundom, mean of two anal.
12) Granophyre of dyke 11, mean of three analyses.

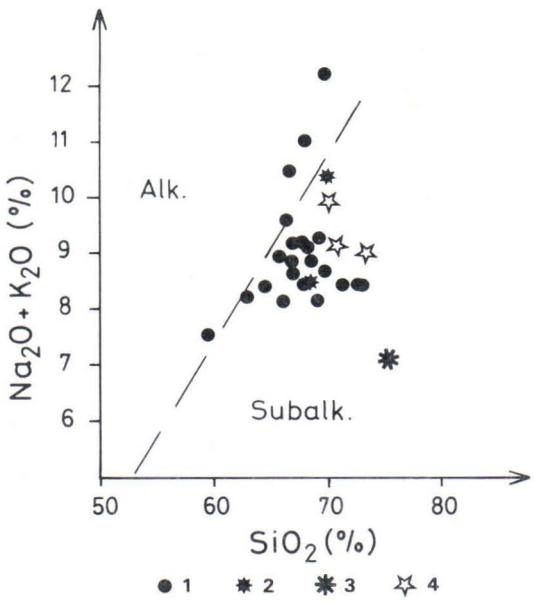

Fig. 10. SiO_2 versus Na_2O + K_2O (wt %) plot of the dykes: 1. Sibbo dykes; 2. spherulite; 3. granophyre; 4. Onas granite. Dividing line after Irvine & Baragar (1971).

etc. diagram (Fig. 12). For comparison, the diagram also shows the Niggli value regression curves for Finnish rapakivi granites as compiled by Haapala (1977).

Study of this diagram reveals that in many respects the dyke rocks are comparable with the rapakivi granites; only the *alk* values of the dyke rocks are slightly higher than the average of the rapakivis. The rock of dyke No. 51 (the composite dyke at Silverlandet), however, shows anomalously high *k, al* and *alk* values and unusually low *fm* and *c*. The rock of dyke No. 47, the middle part of dyke C, also has exceptionally low *k* and *mg* values. It must be emphasised that the analysis of the rock of dyke No. 51 should be taken with caution (see analysis No. 6 in Table 3). Such a high K/Na ratio is not to be expected in the whole rock analysis of a granite. The error may be due to the crude method of analysis, but repeated

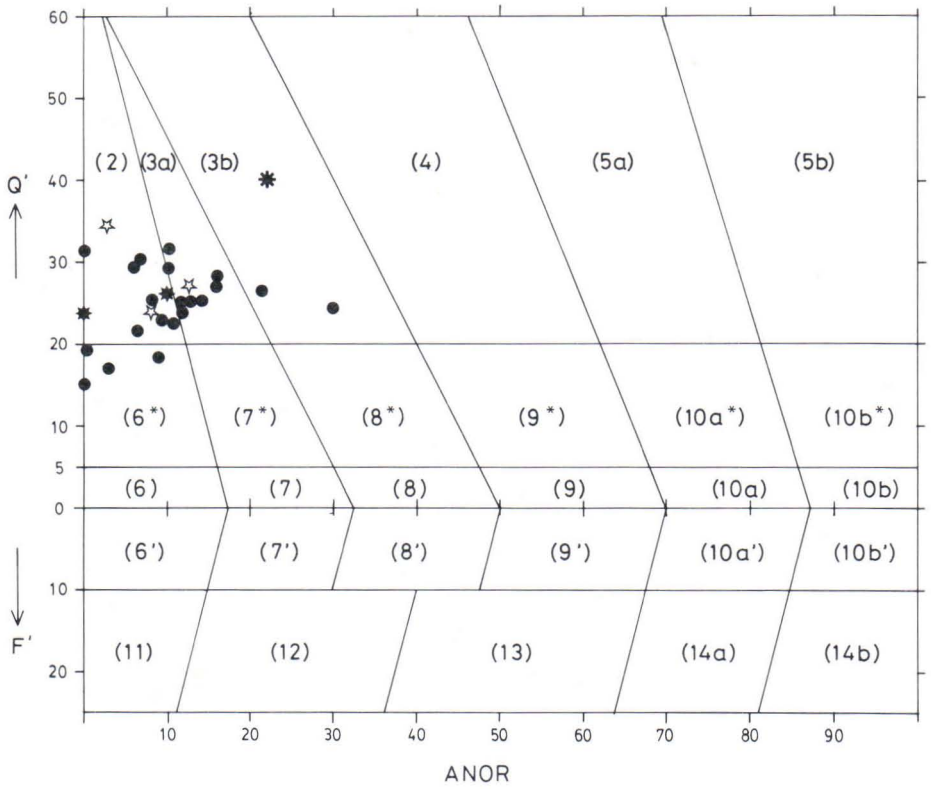

Fig. 11. Q-ANOR diagram of Streckeisen and LeMaitre (1979). All analyses of the dykes plot into the granite-rhyolite fields. Symbols as in Fig. 10.

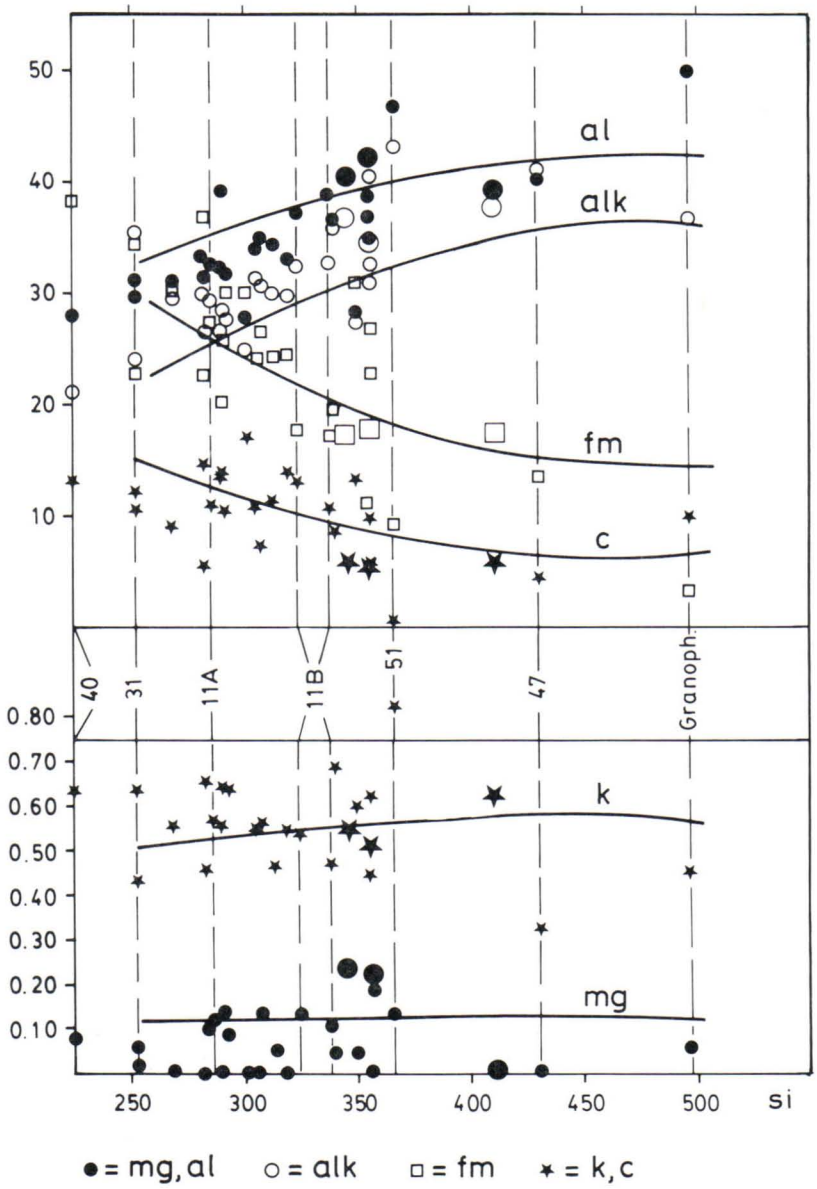

Fig. 12. Niggli diagram of the Sibbo dykes. Curves representing the mean of Finnish rapakivi granites are inserted for comparison (after Haapala 1977). No. 40 is the most Si-poor dyke met with in Sibbo; 11A the groundmass and 11B the contact of the dyke No. 11; No. 47 is the most Si-rich dyke. For comparison the granophyre mean of three analyses of dyke 11 is also given. The bold signs indicate the Onas granite.

Table 4. The mean Niggli values of the Sibbo dykes and the Onas granite compared with the values of different Finnish rapakivi massifs.

	si	mg	k	al	fm	alk	c	N*)
Sibbo dykes	310	0.090	0.57	34.4	23.7	32.2	9.7	18
Onas granite	375	0.15	0.56	40.5	18	36	5.5	3
Laitila massif	408	0.124	0.58	43.6	14.7	34.5	6.8	52
Wiborg ,,	361	0.133	0.56	39.1	20.0	30.9	10.1	37
Salmi ,,	397	0.129	0.55	42.2	18.6	33.4	5.8	81
Vehmaa ,,	373	0.101	0.56	39.0	18.6	33.4	9.0	6
Ahvenisto ,, (Vorma 1976)	386	0.133	0.58	39.9	18.4	33.0	8.7	10
Sahama's ''average'' (Sahama 1945)	375	0.12	0.56	40	18	33	9	37

*)N = number of analyses.

analyses have given about the same results. There is always the possibility that this is an unusually K-felspar-rich part of the rock.

For comparison, the plots of the Niggli values for the granophyre analyses have been inserted in the figure. They clearly differ in their high *si* and *al* values and low *fm* values, showing the lack of minerals other than quartz and felspar.

Table 4 presents the mean Niggli values of the rocks of the Sibbo dykes. For comparison, the table also contains the means of rapakivi granites as compiled by Vorma (1976, p. 31, Table 7). Table 4 shows that the Sibbo dykes tend to be more basic than the Onas granite and the other rapakivi granites. The table also shows lower *mg* and *al* values for the dyke rocks. Curiously, the mean of the three analyses from the Onas granite almost corresponds to Sahama's ''average'' (Sahama 1945).

The differentiation index of Thornton and Tuttle (1960) (DI = sum of normative albite, orthoclase and quartz) varies for the dyke rocks from 70.9 to 94.5, or deleting the two exceptionally high values for dykes No. 51 (DI = 94.5) and No. 47 (DI = 89.9) and the low one for dyke No. 40 (DI = 70.9) the range is 76.7—89.6 with a mean of 81.3 ± 3.3 (11 analyses).

The quartz porphyry and granite porphyry dykes associated with Finnish rapakivi massifs as described or recapitulated by Vorma (1976) and Haapala (1977) are more acid than the Sibbo dykes (see Table 5) with the exception of dyke No. 47, which, as already stated, they much resemble. With the exception of the Sibbo dykes, the dyke rocks mentioned are in general more acid than their presumed rapakivi associates (*cf.* Table 4).

Table 5. Si values of quartz porphyries and granite porphyries and porpfyry dykes associated with rapakivi massifs compared with the values of the Sibbo dykes.

	si (range)	
Sibbo	222—366	(No. 47 = 431)
Onas granite	341—424	
Wiborg	382—445	(Vorma 1971)
Hiidenniemi porphyry (Ruoholampi)	351—365	(Vorma 1975)
Ahvenisto	507	(Savolahti 1956)
Salmi	377—480	(see Vorma 1976)
Hogland and Sommarö	323—453	(Wahl 1947)
Laitila	389—474	(Vorma 1976)
Åland	519	(Sederholm 1934)
Gulf of Bothnia	389—411	(Eskola 1934)
Runsala	354	(Pehrman 1941)
Eurajoki	429	(Haapala 1977)
Bodom	446	*)

*) Unpublished analysis (Prof. M. Härme, Geol. Survey of Finland) of a granite porphyry dyke at Luuk some km to the west of the Bodom granite.

Q-Or-Ab-An-H_2O-System

The granite multicomponent system can be simplified into a four component system if only the minerals quartz and the three felspar components are considered (*e.g.* Winkler 1974, Winkler & Breitbart 1978).

At a given total (H_2O) pressure the tetrahedron outlined by these four components is subdivided by cotectic surfaces into three spaces of primary crystallisation of quartz, plagioclase and K-felspar respectively (*cf.* Winkler & Breitbart 1978, Figs. 1 and 2). The position of the cotectic surfaces and the cotectic line changes as a function of total (H_2O) pressure. The position of the cotectic line has been determined by von Platen (1965) and James and Hamilton (1969). They have established intersecting points of different compositional planes with the cotectic line at 1 and 2 kbar, respectively.

Figure 13 presents a normative *Q-Or-Ab* diagram, where the data from the Sibbo dyke rocks are plotted together with data from the dyke rocks mentioned in Table 5 and from the Finnish rapakivi massifs. The normative *Q, Or* and *Ab* and *Q, Or, Ab* and *An* are recalculated to 100. The normative *An* components of the Sibbo dyke rocks range from 0 to 13.5 or when recalculated to 100, from 0 to 20. Fluorine was not determined in the analyses but minor fluorite does occur in places. This fluorine would consume Ca and thus further lower the normative *An* component.

James and Hamilton (1969) showed that an increasing *An* content would shift the minimum melting point toward the *Q-Or* side. The intersecting points for An_3, An_5, $An_{7.5}$ and An_{10} as projected on the *Q-Ab-Or* plane are included in Fig. 13. If the *An* content were taken into account, almost half the points of the Sibbo dykes swarm would lie in the plagioclase field.

Because fluorite is in part a primary constituent of the rock, an attempt to compensate for fluorine was made for dyke 54 (anal. No. 9 in Table 2). A modal content of 1.5 % fluorite was determined by pointcounter (see Table 1). This equals 0.73 wt % F and would lower the available Ca content in the norm by 0.76 wt %, giving a normative An component of 2.0. Recalculated to 100 in the system *Q-Ab-Or-An,* it would be 2.22 and shift the point to the K-felspar field.

Note that part of the fluorine is secondary. As seen in Fig. 21, fluorite and native metals (Cu and Au) also occur in the corroded parts of the K-felspar phenocrysts. This indicates that a liquid rich in fluorine and with some dissolved metals is responsible for the corrosion. The calcium needed for the formation of fluorite may be assumed, at least partly, to originate from the very anorthite-rich plagioclase within the phenocrysts (see Fig. 5).

On the other hand, studies on the effect of fluorine upon the isobaric minima and the crystallisation of granitic magma (*e.g.* von Platen 1965; Anfilogov *et al.* 1973; Kovalenko *et al.* 1971; Kovalenko 1973; Manning *et al.* 1980) demonstrate that a small addition of fluorine to a granite-H_2O mixture at constant pressure markedly lowers the crystallisation temperatures. Von Platen (1965) and Manning *et al.* (1980) also show that the isobaric minima shift away from the quartz corner, *i.e.* increase the field of quartz. According to von Platen *(op.cit.),* the field shift is towards the *Or* corner, but Manning *et al. (op.cit.)* have demonstrated that the shift is towards the *Ab* corner.

Haapala (1977) has applied this to the Eurajoki rocks, and he suggests that the scattering of the compositional point of the topaz-bearing quartz porphyry dyke sample towards the *Ab* corner in relation to the other samples of Väkkärä granite analysed could be due to increased fluorine content in the residual magma.

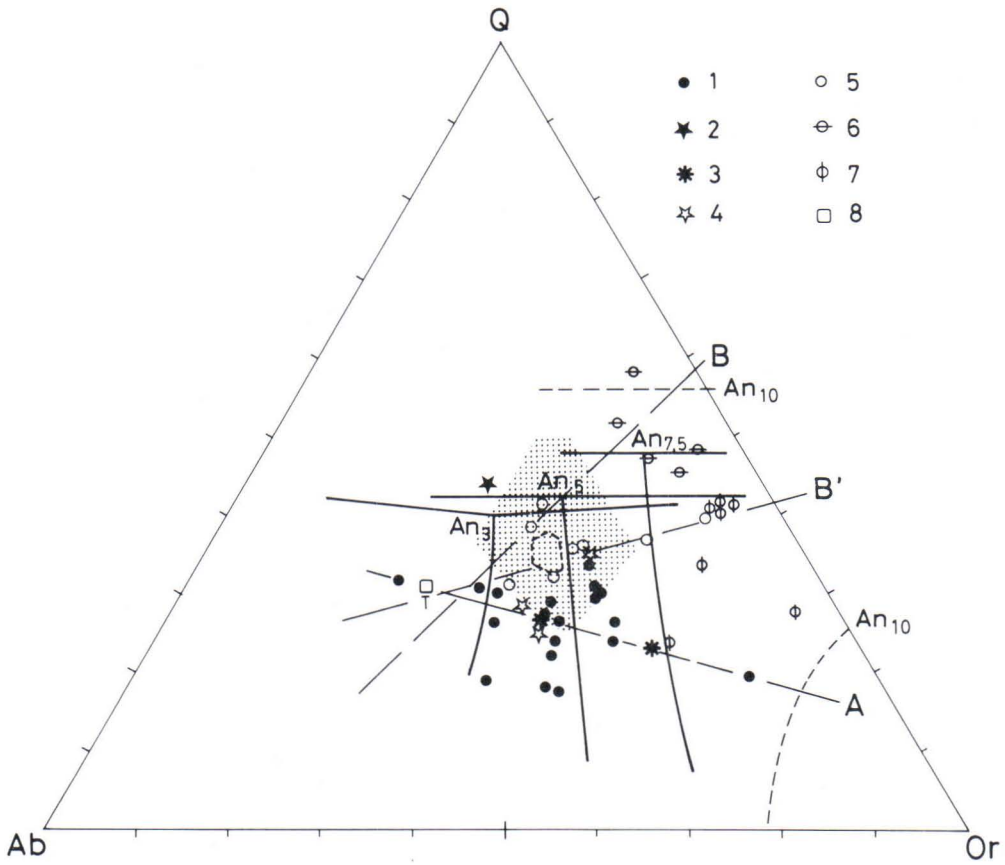

Fig. 13. Normative albite—orthoclase—quartz diagram of the dykes compared with the experimentally determined phase diagrams and minima in the An-bearing systems (under 1 kbar water vapour pressure) of James and Hamilton (1969) and with the rapakivi granites of Finland (shaded area). The demarcated area represents the mean compositions of the rapakivi granite massifs of Finland. Differentiation path of the magma: B' using the analyses of Wahl (1947) on the quartz porphyries of Hogland and Sommarö or B'' using the data of Lemberg (1867). Line A represents the compositional spread of the Sibbo dykes. 1. Sibbo dykes; 2. granophyre; 3. spherulite; 4. Onas granite; 5. porphyry dykes from the Wiborg rapakivi massif (after Vorma 1976); 6. quartz porphyries from Hogland and Sommarö (after Wahl 1947); 7. quartz porhyries from Hogland (after Lemberg 1867); 8. porphyry dyke from the Tarkki granite (after Haapala 1977).

Though there is an obvious scatter of the dyke points in Fig. 13, they cluster, however, at a somewhat *Q*-poorer area than the normal rapakivis and the other quartz porphyries and granite porphyries or porphyry dykes connected with the rapakivi massifs.

There is no clear trend towards the *Ab* or *Or* corners in the analysed samples in which fluorite has been encountered (samples 11, 31 and 54). Conclusions cannot therefore be drawn from these few points on the influence of fluorine. The low SiO_2 content of these dyke rocks as against that of the Onas granite implies that the dyke rocks represent an earlier differentiation stage than the Onas granite.

Examination of Fig. 13 reveals that the Sibbo dykes vary in composition, as shown by line A. Line B is more or less consistent with

the results of differentiation obtained by Tuttle and Bowen (1958). Because the analyses of quartz porphyries from Hogland and Sommarö (two islands in the Gulf of Finland, south of the Wiborg rapakivi massif) are very scattered there may be another trend, too, as shown by line B'.

Be that as it may, the compositional trend of the emplaced magmas in southern Finland is towards the *Q-Or* side of the diagram.

Trace elements

The results of the trace element analyses (XRF method) are listed in Table 2. The lanthanoids (neutron activation) determined on the three samples, Nos. 11, 54 and the Onas granite, are given in Table 6.

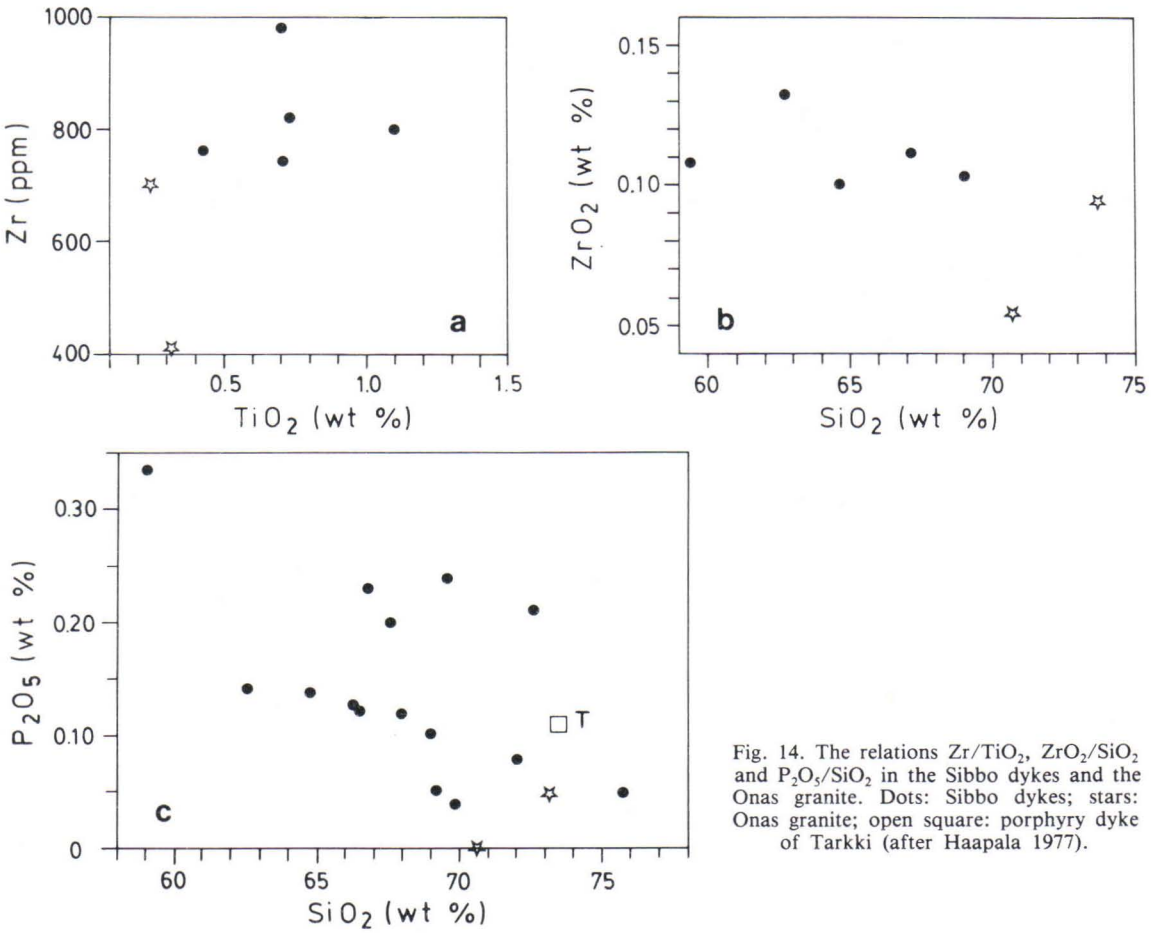

Fig. 14. The relations Zr/TiO_2, ZrO_2/SiO_2 and P_2O_5/SiO_2 in the Sibbo dykes and the Onas granite. Dots: Sibbo dykes; stars: Onas granite; open square: porphyry dyke of Tarkki (after Haapala 1977).

P, Ba, Rb, Zr

Some correlation diagrams are compiled in Fig. 14. The plot of P_2O_5 versus SiO_2 demonstrates that P_2O_5 increases with decreasing SiO_2. The only phosphorus mineral encountered is apatite and there is no apatite concentration in any of the dykes. The mineral

analyses, however, show that phosphorus has been encountered in the mafic minerals of the more basic dykes in particular, probably thus giving rise to the phosphorus enrichment in them.

In the Onas granite the P_2O_5 content is very low (0—0.05 wt %). This is considerably less than that of Sahama's standard mixture, *viz.*, 0.18 wt % (Sahama 1945). On the other hand, Sahama's value is more in accord with the P content of the dyke rocks.

Rb_2O and BaO do not correlate with K_2O. Ba is considered to be enriched in early-formed potassium minerals (see discussion on p. 26 in connection with the K-felspar phenocrysts). The Rb:K ratio should increase with increasing differentiation, but no such trend is seen here either. Sahama's standard mixture contains 0.16 wt % Rb_2O and the values for Onas and the Sibbo dykes are far below this.

On the other hand, the diagram (Fig. 14 b) shows the clear correlation between ZrO_2 and SiO_2. The ZrO_2 content is markedly higher in the Sibbo dyke rocks than in the Onas granite or the rapakivi granites (see Vorma 1976, p. 64). According to Poldervaart (1956), zircon crystallises at an early stage from a granitic or dioritic magma, and Murthy (1958) suggests that zircon crystallises during a very short period at an early stage of a granite intrusion. Vlasov (1968), too, states that Zr is confined to the earlier basic differentiates of a granitic intrusion. The plot of Zr/TiO_2 (Fig. 14 a) shows a clear positive correlation, except for one point of the Onas granite. Both these zirconium correlation diagrams show a differentiation series with the Onas granite as final stage. This is one of the factors demonstrating that the dykes are not in a mother-daughter relation to the Onas granite massif; other factors will be discussed in the following.

RE elements

Rare earth elements in granitic rocks have been the subject of numerous investigations in recent decades (*e.g.* Emmermann *et al.* 1975). The findings may be summed up as follows:

1) The REE content increases during magmatic differentiation.
2) The lighter REE *i.e.* La-Sm are generally enriched relative to the heavier REE *i.e.* Gd-Lu.
3) Eu shows anomalous behaviour in that in some granites, *e.g.* many alkaline and peralkaline ones ((K + Na)/Al> 1), it is considerably more depleted than the neighbouring Sm and Gd, whereas subalkaline granites frequently have a smooth concentration distribution of REE (Bowden & Whitley 1974). Consequently, there are two basic types of frequency distribution of REE in granites, a smooth one with a general decrease in concentration from La to Lu, and another one with a negative Eu anomaly.

Table 6. Rare earth abundances of Sibbo granite porphyries and Onas granite (ppm). Numbers in brackets correspond to these in Table 2.

Sample		La	Ce	Nd	Sm	Eu	Tb	Tm	Yb	Lu	REE	(La/Yb)e.f.
Onas	(1)	159	291	160	24	5.7	3.6	1.2	8.5	0.74	774	10.8
Onas	(3)	90	160	80	20	3.5	2.2	—	4.9	0.3	402	10.8
11	(8)	107	199	99	15	3.8	2.6	1.2	8.0	0.71	488	7.9
54	(9)	194	382	192	35	2.5	4.8	1.7	14.5	1.27	935	7.9

Onas (3) from Nieminen and Yliruokanen (1974) (determ. by spark source mass spectrometry).

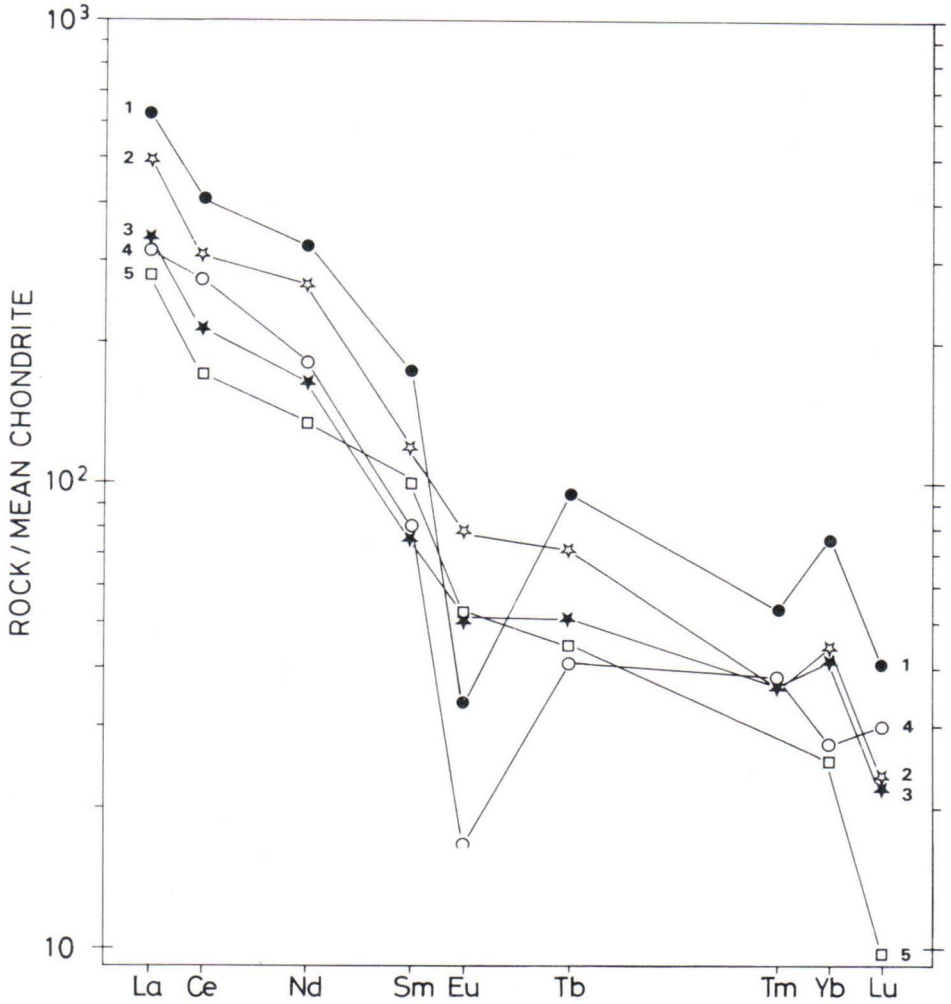

Fig. 15. Chondrite normalised REE distribution patterns in the Sibbo dykes and the Onas granite compared with a quartz porphyry dyke from the Wiborg rapakivi massif. 1. dyke No. 54; 2. Onas granite; 3. dyke No. 11; 4. quartz porphyry from the Wiborg rapakivi (Vorma 1976, anal. 51); 5. Onas granite (Nieminen & Yliruokanen 1974).

The contents of the individual REE and the total REE of the Sibbo dyke rocks and the Onas granite are given in Table 6. The chondrite normalised patterns are given in Fig. 15. For normalisation purposes the values of Herrmann (1970) were used. The total REE were calculated by interpolating the values for the elements not determined from these curves. As a measure of the degree of fractionation (enrichment factor, e.f.) (Emmermann *et al.* 1975) of the REE in the different types of granite the chondrite normalised La/Yb ratio is used and given as (La/Yb)e.f.

The (K + Na)/Al ratio implies that the Sibbo dykes lie on both sides of the alkaline—subalkaline border. As discussed before (p. 13) and according to the plot in Fig. 10, the majority of the dykes, however, are subalkaline.

Two types of curve are revealed by the REE distribution patterns of the dykes and the Onas granite shown in Fig. 15. The two curves representing the Onas granite resemble each other very much and also the pattern for dyke No. 11, *i.e.* they show a smooth concentration distribution curve with a general decrease from La to Lu. The total REE content in dyke No. 11 is 488 ppm and in the Onas granite 402 and 774 ppm, respectively. The REE pattern of dyke No. 54, on the other hand, is characterised by marked Eu depletion while the content of total REE increases to 935 ppm. The trend of the pattern, however, is the same as for the others. The (La/Yb)e.f. is 7.9 for the both dyke rocks and about 11 for the Onas granite. The enrichment factor again shows that the Onas granite is more differentiated than the Sibbo dykes.

There is no connection between the total REE and the major element chemistry of the rocks. A comparison with the REE patterns for rapakivi given by Vorma (1976, p. 74—76) reveals that the rapakivis all show an anomalous Eu depletion as does the granite porphyry dyke reported by Vorma *(op.cit.)*. For comparison, the REE pattern for this dyke is also given in Fig. 15.

The main features of the chondrite normalised REE patterns of the samples studied (Fig. 15) are:

1) The samples are enriched in light REEs, the chondrite normalised values for the lightest REEs being consistently higher (by about one order of magnitude) than the heaviest, (La/Yb)e.f. = 8 (Table 6).
2) There is a striking negative Eu anomaly in sample No. 54. This sample plots in the subalkaline field of Fig. 10, and thereby constitutes an exception to the general rule of Bowden and Whitley (1974).
3) The patterns of Onas granite closely resemble that of dyke No. 11.
4) The Onas granite is more differentiated than the Sibbo dykes.

The apparently negative Ce anomalies are believed to be due to analytical factors.

MINERAL CHEMISTRY

Chemical compositions of the constituent minerals were determined by electron microprobe. The results are given in Tables 7, 9 and 10.

Plagioclase

The An content of the plagioclase phenocrysts ranges from An_0 to An_{73}. Albite phenocrysts are scarce. The main compositions, however, range from oligoclase to labradorite. Albite may also be met with in K-felspar phenocrysts. Representative plagioclase analyses are given in Table 7a.

Chemical zoning within the plagioclase phenocrysts is common. Typically two types of zoning occur: one shows a general decrease in the Ca/Na ratio from core to margin, but with reverse jumps. According to Homma (1936, Fig. 10), this type should be classified as normal-oscillatory normal zoning. The other type shows first a slight increase in the Ca/Na ratio and then a slight decrease, with the An and Ab contents, however, being generally even. Homma *(op. cit.)* would call this wavy-oscillatory even zoning. The potassium content displays jumps, but with a general increase

Table 7a. Selected microprobe analyses of Sibbo dyke plagioclase (wt. %).

	1	2	3	4	5	6	7
SiO_2	59.72	56.89	57.58	55.92	59.42	58.60	56.80
TiO_2	0.03	0.18	0.09	0.28	0.02	0.07	0
Al_2O_3	25.61	26.91	26.12	24.49	26.97	26.29	26.96
FeO *	0.07	0.40	0.22	4.37	0.03	0.25	0.36
MnO	0.03	0.08	0	0.07	0	0.01	0.03
MgO	0	0	0.01	0.03	0	0.02	0
CaO	6.82	9.60	9.50	9.41	8.07	8.38	9.10
Na_2O	8.98	7.10	7.11	6.28	7.64	7.12	7.36
K_2O	0.12	0.14	0.29	0.46	0.16	1.00	0.10
P_2O_5				0.03			
Total	100.38	101.30	100.92	100.44	102.31	101.74	100.71
Number of ions on the basis of 32 oxygens:							
Si	10.562	10.154	10.298	10.116	10.406	10.386	10.181
Ti	0.004	0.024	0.012	0.039	0.003	0.009	0
Al	5.338	5.661	5.506	5.307	5.567	5.492	5.695
Fe	0.010	0.060	0.033	0.672	0.004	0.037	0.054
Mn	0.004	0.012	0	0.011	0	0.002	0.005
Mg	0	0	0.003	0.008	0	0.005	0
Ca	1.292	1.836	1.820	1.854	1.514	1.591	1.748
Na	3.079	2.457	2.465	2.239	2.594	2.447	2.558
K	0.027	0.032	0.066	0.108	0.036	0.226	0.023
P				0.005			
O	32.000	32.000	32.000	32.000	32.000	32.000	32.000
Ab	70.00	56.81	56.65	53.30	62.60	57.38	59.09
Or	0.62	0.74	1.52	2.57	0.86	5.30	0.53
An	29.38	42.45	41.83	44.13	36.54	37.32	40.38

* Total iron as FeO

1) Plagioclase phenocryst, dyke No. 27, Gumbostrand (x = 6683,64 y = 571,46)
2) ,, phenocryst, dyke No. 3, Bisaträsk, Vanda. (x = 6688,43 y = 562,97).
3) ,, groundmass, ,,
4) ,, phenocryst, dyke No. 31, Vallkulla, Sibbo kyrkoby
5) ,, groundmass, ,,
6) ,, phenocryst, dyke No. 11, Östersundom
7) ,, groundmass, ,,

towards the margin; at the rim it shows a marked jump. Table 7c gives results of analyses on a chemically zoned felspar phenocryst.

The zonal structures may indicate that the magma was subjected to changes in its chemical and physical conditions before intrusion.

In the groundmass plagioclase, the An content varies from An_0 to An_{60}, *i.e.* from albite to labradorite, albite, however, being very abundant. The potassium content in the groundmass plagioclase is lower than in the rim of the phenocrysts, indicating that the crystallisation period of the rim was different from that of the groundmass.

K-felspar

Table 7b gives some representative microprobe analyses of K-felspar. The potassium content seems to be somewhat higher in the groundmass K-felspar than in the phenocrysts. Optical zoning is not seen normally, but chemical zoning, shown by Ba, does occur (see

Table 7b. Selected microprobe analyses of K-felspar from the Sibbo dykes (wt. %).

	1	2	3	4	5	6	7
SiO_2	63.46	63.66	64.17	65.26	65.96	63.34	63.04
TiO_2	0.63	0.08	0.03	0	0	0.03	0
Al_2O_3	19.30	19.90	18.49	19.19	20.10	20.61	19.33
FeO *	0	0	0	0.05	0.01	0.06	0.14
MnO	0	0	0	0.02	0.03	0	0.03
MgO	0	0.01	0	0	0	0	0
CaO	0.01	0.49	0.14	0	0	0	0.03
Na_2O	0.62	0.66	0.69	0.71	0.71	0.95	0.53
K_2O	15.88	13.82	13.24	14.42	14.42	13.49	16.46
Total	99.90	98.62	96.76	99.65	101.23	98.48	99.56
Number of ions on the basis of 32 oxygens:							
Si	11.757	11.801	12.055	11.975	11.900	11.734	11.767
Ti	0.088	0.011	0.004	0	0	0.004	0
Al	4.214	4.348	4.094	4.150	4,274	4.500	4.252
Fe	0	0	0	0.008	0.002	0.009	0.022
Mn	0	0	0	0.003	0.005	0	0.005
Mg	0	0.003	0	0	0	0	0
Ca	0.002	0.097	0.028	0	0	0	0.006
Na	0.223	0.237	0.251	0.253	0.248	0.341	0.192
K	3.753	3.268	3.173	3.375	3.319	3.188	3.919
O	32.000	32.000	32.000	32.000	32.000	32.000	32.000
Ab	5.60	6.58	7.28	6.96	6.96	9.67	4.66
Or	94.35	90.71	91.90	93.04	93.04	90.33	95.20
An	0.05	2.70	0.82	0	0	0	0.15

* Total iron as FeO

1) Microcline, Onas granite
2) K-felspar phenocryst, dyke No. 44, Stor Annas sten (x = 6692,10 y = 573,54)
3) ,, groundmass, ,,
4) ,, phenocryst, dyke No. 9, Ringberga
5) ,, groundmass, ,,
6) ,, phenocryst, dyke No. 3, Bisaträsket, Vanda
7) ,, groundmass, ,,

below). Narrow albite zones occasionally occur in K-felspar phenocrysts. Two analyses of such a pair are given in Table 7c, points 5 and 6.

The distribution of Ba in the K-felspar phenocrysts of the Sibbo porphyry dykes was studied by electron microprobe. It was verified that the phenocrysts usually have a core with a rather even Ba content and a Ba-poorer shell with inclusions of quartz and plagioclase (albite) (Fig. 16). The reverse is true in some phenocrysts, however; in these there is a Ba-poorer core with a continuous increase in Ba towards the margin (Fig. 17), evidently indicating diffusion of Ba into the phenocryst.

Another interesting point in the Sibbo dykes is that the Ba content varies between the cores of different phenocrysts. According to Mehnert and Büsch (1981), Ba begins to concentrate in the cores of megacrysts during the earliest stages of granite development. The Ba content changes during the following stages of crystallisation and zonation develops in the shells.

Winkler and Schultes (1982) have shown that alkali felspar phenocrysts may form at each stage of the crystallisation history. Phenocrysts may thus develop with varying Ba contents, depending on the time at which they began to develop. This may be one explanation for the varying Ba contents of the phenocrysts in the Sibbo dykes.

Table 7c. Selected microprobe analyses of chemically zoned felspar phenocrysts from the dykes of Sibbo (wt. %).

	1	2	3	4	5	6
SiO_2	57.64	56.81	64.94	63.07	63.43	65.03
TiO_2	0.06	0.08	0.03	0.03	0.04	0
Al_2O_3	26.55	25.53	21.05	21.07	19.57	22.35
FeO *	0.27	0.27	0.26	0.05	0.10	0.15
MnO	0	0	0	0	0	0.03
MgO	0	0	0.01	0	0	0
CaO	8.63	8.15	1.10	1.34	0	1.14
Na_2O	4.99	3.74	4.13	2.61	0.23	11.46
K_2O	3.05	5.64	7.79	9.45	16.57	0.05
P_2O_5			0.13	0	0.04	0.01
Total	101.19	100.22	99.44	97.62	100.44	100.22
Number of ions on the basis of 32 oxygens:						
Si	10.330	10.385	11.688	11.635	11.756	11.427
Ti	0.008	0.011	0.004	0.004	0.006	0
Al	5.608	5.500	4.465	4.581	4.257	4.629
Fe	0.040	0.041	0.039	0.008	0.015	0.022
Mn0	0	0	0	0	0.004	
Mg	0	0	0.003	0	0	0
Ca	1.657	1.596	0.212	0.265	0	0.215
Na	1.734	1.326	1.441	0.934	0.083	3.904
K	0.697	1.315	1.789	2.224	3.918	0.011
P			0.020	0	0.006	0.001
O	32.000	32.000	32.000	32.000	32.000	32.000
Ab	42.41	30.29	41.87	27.28	2.07	94.53
Or	17.06	31.50	51.97	64.98	97.93	0.27
An	40.53	38.22	6.16	7.74	0	5.20

* Total iron as FeO

1—4 A felspar phenocryst from Fårholmen, (1—2 are plagioclase-dominant central part, 3—4 alkali-dominant outer part of the phenocryst. Note that the potassium content increases from point 1 to 4) 5 and 6. Small alkalifelspar phenocryst, dyke No. 51, Silverlandet.

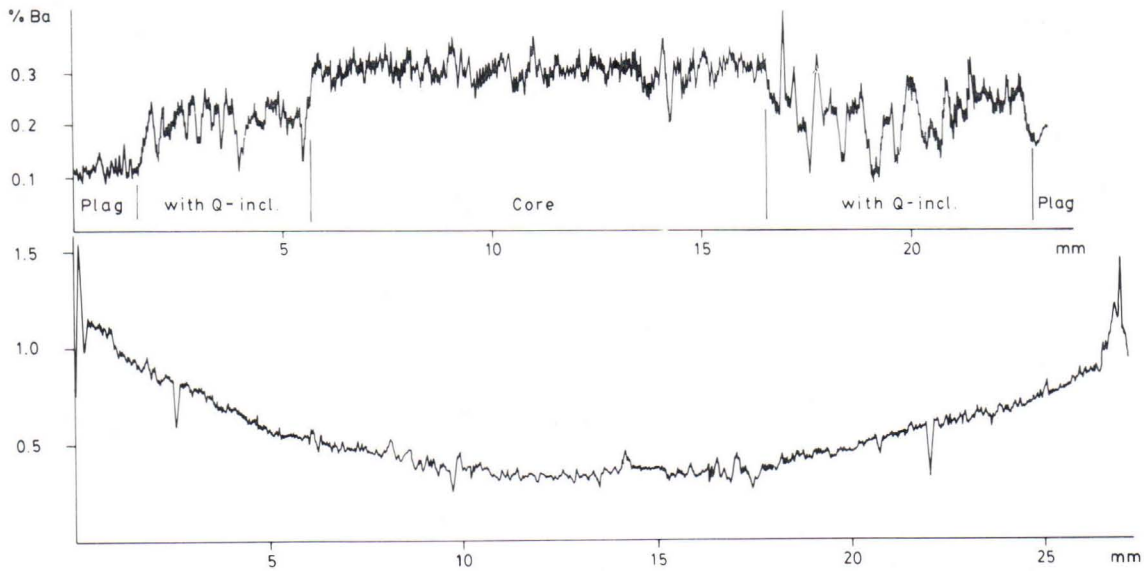

Figs. 16 and 17. Line scanning profiles of the Ba content across two K-felspar phenocrysts of dyke Nos. 44 and 53. The traverse of No. 44 corresponds to the crystal shown in Fig. 3. The core of the crystal has a higher Ba content than the rim or the zone of intergrown quartz. The traverse in Fig. 17 shows the effect of Ba diffusion into the phenocrysts. The Ba content is 0.3 wt % at the minimum in the centre of the crystals and 0.9 wt % at the margins. The Ba peak right at the rim rises to 1.5 wt %.

X-ray investigation of K-felspar

X-ray powder patterns were recorded for phenocrysts from several dyke rocks and from a few groundmass samples with a Phillips wide-angle diffractometer by means of Ni-filtered Cu radiation and an internal quartz standard.

Corrected reflections for $\bar{2}04$, 060, 131 and $1\bar{3}1$ were used. The degree of Al/Si ordering is visible in the plot according to Stewart and Wright (1974) of d_{060} versus $d_{\bar{2}04}$ (Fig. 18). The majority of the K-felspar phenocrysts cluster near the corner of maximum microcline, but the whole range from orthoclase to maximum microcline does occur. The few measurements obtainable from the groundmass also show the range from orthoclase to microcline.

More information about the structural state was obtained by calculating the degree of triclinity as outlined by Goldsmith and Laves (1954) by measuring the separation $d_{131} - d_{\overline{131}}$ of the X-ray powder patterns (triclinity $\Delta = 12.5(d_{131} - d_{\overline{131}})$. The results are given in Table 8.

The degree of Al/Si ordering in felspars may preserve a record of the conditions of rock formation. Equilibrium ordering in most geological environments is imperfectly approached at the best and it is questionable whether alkali felspar in nature ever forms directly with an amount of Al/Si order that corresponds to thermodynamic equilibrium under the conditions of formation. On heating, the lowest temperatures at which significant Al/Si diffusion occurs are in the range of

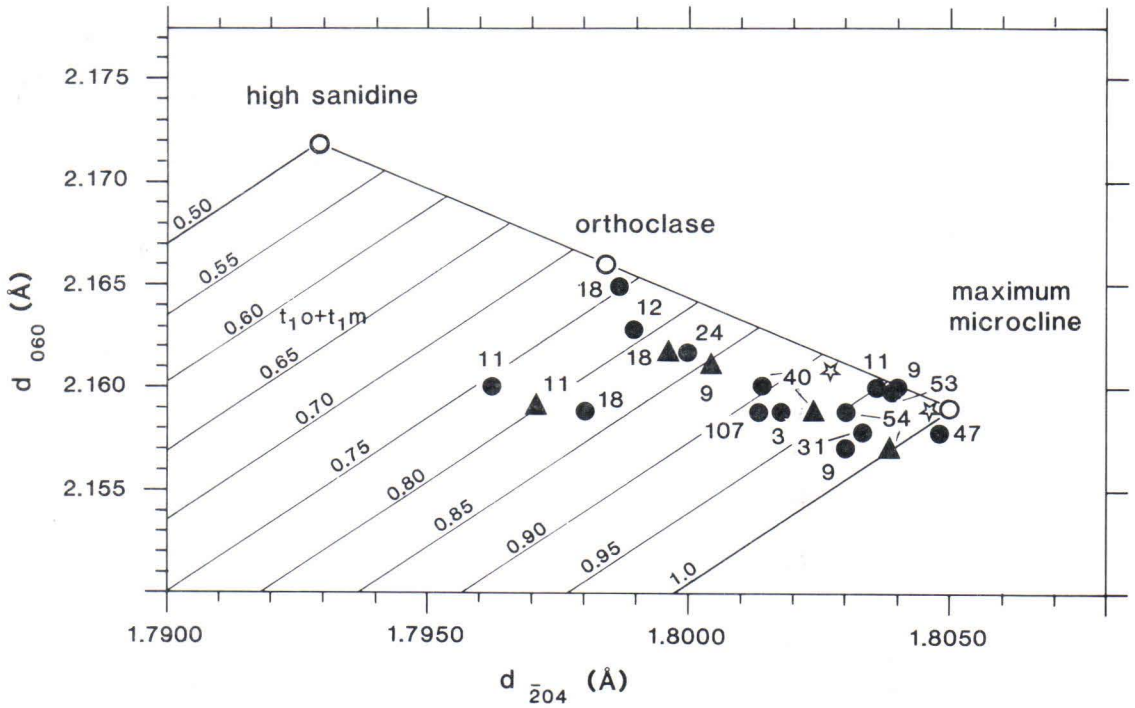

Fig. 18. A plot of observed $d_{\overline{204}}$ values against the observed d_{060} values for K-felspar phenocrysts and groundmass from the Sibbo dykes. Contours modified after Stewart and Wright (1974). Specimen numbers as in Fig 1. Circles: phenocrysts; triangles: groundmass; stars: Onas granite.

Table 8. Triclinity and $2t_1$ of K-felspar from the Sibbo dykes calculated using the formula $\Delta = 12.5(d_{131} - d_{\overline{131}})$ of Goldsmith and Laves (1954) and the Al/Si order-disorder diagram of Stewart and Wright (1974).

Dyke No.	triclinity	$2t_1 = t_1o + t_1m$	
3	0.94	0.92	phenocryst
9	0.94	0.97	,,
9	0.65	0.86	groundmass
11	0.94	0.94	phenocryst
11	0.21	0.76	,,
11	n.m.	0.79	groundmass
12	0.0	0.78	phenocryst
18	0.0	0.74	,,
18	0.35	0.82	groundmass
31	0.97	0.97	phenocryst
40	0.85	0.88	,,
40	0.93	0.93	groundmass
47	0.98	1.00	phenocryst
53	0.91	0.96	,,
54	0.98	0.95	,,
54	1.00	1.00	groundmass
Fårholm (107)	0.93	0.91	phenocryst
Onas granite	0.86	0.91—0.98	

n.m. = not measurable

300°—400° C, were maximum microcline seems to remain stable (Stewart & Wright 1974). The upper temperature limit of maximum microcline stability is estimated to be 375° ± 50°C (Wright 1967, p. 130—131). Microcline is unstable at temperatures above 600°C (Guidotti *et al.* 1973). Stewart and Wright (1974) suggest that monoclinic felspars with $2t_1$ = 0.75—0.80 are the stable Al/Si configuration of the K-felspars of the K-felspar—sillimanite assemblage according to Guidotti *et al. (op. cit.,* p. 707) representing the thermal maximum (655° ± 20°C).

Stewart and Wright (*op.cit.*) suggest that the more ordered monoclinic samples and the triclinic samples of this assemblage represent ordering that occurred in response to falling temperature, and the presence of alkali-rich solutions and other factors that effect ordering kinetics.

The upper-medium and high grade metamorphism, where partial melting buffers the temperature that can be attained, and the last stage of crystallisation of granitic magma are probably both in the range 625°—750°C. Under such conditions the primary K-felspar is orthoclase with $2t_1$ = 0.8 ± 0.1. It apparently forms directly, or if the felspar formed is more disordered it becomes ordered immediately (Stewart & Wright *op.cit.*).

The stable configuration of K-felspar in the intermediate temperature range 400°—600° C is not known to the above authors (*op.cit.,* p. 369) and a field of stability for intermediate microcline cannot be defined. Neither is the lower limit of orthoclase stability known.

Although there are many objections to the two-felspar thermometer, it was still applied to the dykes studied. According to the method and graphs outlined by Stormer (1975) and by Whitney and Stormer (1976, 1977), the measurements of the groundmass felspars give a crystallisation temperature of <400°C. The groundmass felspars are presumed to have crystallised together and therefore to give reliable results. If it is accepted that the alkali felspar and the plagioclase in the phenocrystic assemblages crystallised simultaneously, some indication would be given about the crystallisation temperature. Measurements from such assemblages give temperatures of 530°—700°C.

The occurrence of orthoclase in the groundmass is admittedly a consequence of rapid crystallisation when a hot magma intruded in a cold environment. There was no time for Al/Si ordering. The pressure must have dropped considerably when the magma flowed into the narrow fractures, changing the equilibrium conditions. Some of the phenocrysts may also have crystallised in situ in the dyke (see discussion on p. 9).

The microcline phenocrysts may have formed in either of two ways: 1) they crystallised at a very late stage, probably just after intrusion, from an undercooled magma, or 2) the K-felspar formed was ordered later in response to falling temperature.

Biotite

Biotite is the principal mafic mineral and occurs in all dykes. The content varies little (cf. Table 1). It is present in exceptionally small amounts in the dyke at Spjutsund (10 vol %) but ranges from 18 to 27 vol % in the other dykes.

Representative microprobe analyses of the dyke biotite are given in Table 9. Wet chemical analyses of biotite were not performed, and the investigation was therefore somewhat hampered by the limitations of the electron microprobe (*e.g.* light element analyses, oxidation state).

Neverthless, the results of the microprobe analyses show that the biotite has a very high Fe/(Fe + Mg) ratio and a composition near that of siderophyllite. The highest TiO_2 content (4—5 wt %) was in the biotite from dyke No. 40. The TiO_2 content of the whole rock of this dyke was also high, being the highest of any of the Sibbo dyke rocks, or 1.1 wt % (see Table 2, anal. 4).

According to Nockolds (1947), the compositional variation of biotite may be visualised in an FeO-Al_2O_3-MgO diagram (Fig. 19). The three fields I-III show biotite compositions

Table 9. Selected microprobe analyses of dyke biotite and chlorite (wt. %).

	1	2	3	4	5	6	7	8
SiO_2	32.17	32.83	34.04	33.84	35.24	33.24	26.45	23.71
TiO_2	2.03	1.98	3.31	2.45	2.16	3.65	0.28	0.61
Al_2O_3	16.21	14.89	14.18	16.55	16.06	16.98	22.06	17.85
FeO*	36.52	35.90	36.99	33.48	33.53	31.77	36.78	43.04
MnO	0.24	0	0.33	0.09	0.28	0.37	0.43	0.32
MgO	0.42	0.70	1.52	1,58	1.84	1.88	0.19	0.63
CaO	0.08	0.19	0	0.05	0	0.02	0	0.52
Na_2O	0.06	0.04	0	0.04	0.06	0.05	0.02	0.02
K_2O	7.93	9.37	8.42	9.50	8.45	9.84	0.03	0.53
P_2O_5	0	0.06	0	0	0	0.08	0	0.18
Total	95.66	94.96	98.79	97.58	97.62	97.88	86.24	87.41
Number of ions on the basis of 22 oxygens;								28 oxygens:
Si	5.336	5.371	5.467	5.426	5.594	5.292	5.984	5.607
Ti	0.253	0.251	0.400	0.295	0.258	0.437	0.048	0.108
Al	3.169	2.961	2.684	3.128	3.005	3.186	5.882	4.975
Fe	5.066	5.066	4.968	4.490	4.451	4.230	6.959	8.513
Mn	0.034	0	0.045	0.012	0.038	0.050	0.082	0.064
Mg	0.104	0.176	0.364	0.378	0.435	0.446	0.064	0.222
Ca	0.014	0.034	0	0.009	0	0.003	0	0.132
Na	0.019	0.013	0	0.012	0.018	0.015	0.009	0.009
K	1.678	2.017	1.725	1.943	1.711	1.998	0.009	0.160
P	0	0.009	0	0	0	0.011	0	0.036
O	22.000	22.000	22.000	22.000	22.000	22.000	28.000	28.000
mg	2.0	3.4	6.8	7.7	8.8	9.4	0.9	2.5

* total iron as FeO, mg = 100 Mg/(Mg + Mn + Fe)

1) Biotite, dyke No. 44, Stor Annas sten
2) ,, ,, ,, 31, Vallkulla, Sibbo kyrkoby.
3) ,, ,, ,, 9, Ringberga, Östersundom.
4) ,, ,, ,, 107, Fårholmen
5) ,, ,, ,, 12, Östersundom (x = 6683,25 y = 567,92)
6) ,, ,, ,, 40, Road and railway cutting on the Nickby—Sköldvik road, parish of Borgå.
7) Chlorite, ,, ,, 51, Silverlandet
8) ,, ,, ,, 44, Stor Annas sten

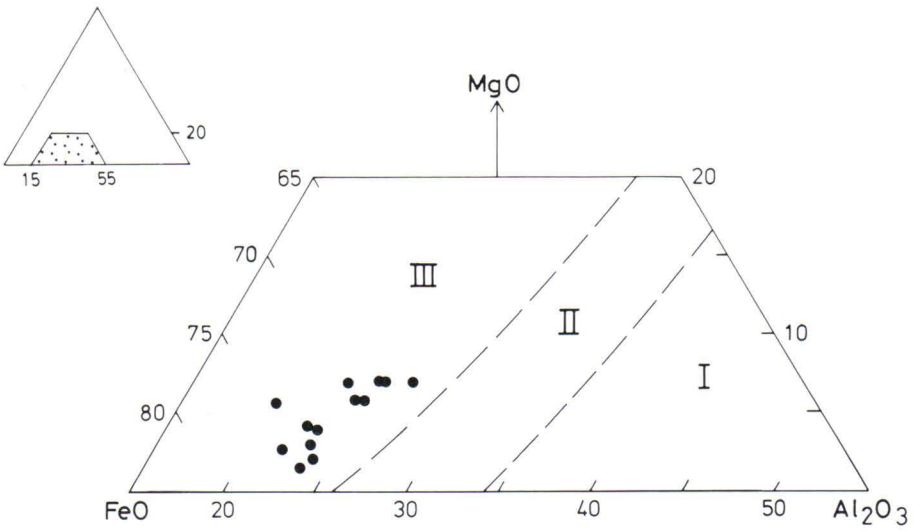

Fig. 19. Proportions of MgO, FeO(total) and Al_2O_3 wt % in biotite from the Sibbo dykes. The biotite of all the dykes plots into the part of field III where they should be associated with hornblende. Field contours (after Nockolds 1947) divide the biotite compositions for different mineral associations (see text).

together with different mafic mineral associations as follows:

I biotite associated with muscovite, topaz, etc.
II biotite alone
III biotite associated with hornblende, pyroxene and/or olivine

Biotite falling in the more iron-rich corner of field III is associated with hornblende, and more Mg-rich biotite is associated mainly with pyroxene and/or olivine.

The Sibbo dyke biotites all plot into the FeO rich part of field III (association with hornblende). This is consistent with microscope observations. Pyroxene or olivine have been encountered very rarely in only two dykes: in the branch of dyke No. 11 shown in Fig. 2 and in dyke No. 18. Hornblende, on the other hand, follows biotite in almost all dykes.

Most of the published biotite analyses for Finnish rapakivi granites also plot in field III (see Simonen & Vorma 1969; Haapala 1977). Exceptions are the biotites of topaz-bearing types (field I), the contact type and the equigranular type (border between fields I and II) of the Väkkärä granite (Haapala *op.cit.*).

Plagioclase and biotite are the two original minerals of the dykes that are most susceptible to alteration. Microprobe analyses indicate that biotite, on altering to chlorite, loses much Ti, Si and practically all K but that Al and Fe tend to increase (see Table 9).

Hornblende, pyroxene and fayalite

Together with biotite, hornblende constitutes the only noteworthy mafic mineral in the dykes (6—14 vol % when present). In the dykes numbered 44, 46, 45, 51, 53 and 54 it was not seen at all in the thin sections studied; biotite constitutes the only mafic mineral in these dykes.

The representative microprobe analyses are

Table 10. Selected microprobe analyses of hornblende and orthoferrosilite from the Sibbo dykes (wt. %).

	1	2	3	4	5	6	7
SiO_2	38.42	37.61	37.96	39.43	40.26	46.42	46.84
TiO_2	0.53	0.31	1.20	1.03	1.55	0.91	0.35
Al_2O_3	9.30	13.96	11.60	13.05	9.67	1.57	0
FeO*	31.56	29.88	33.23	30.34	32.77	41.49	43.44
MnO	0.16	0.49	0.49	0.13	0.59	0.85	0.75
MgO	0.56	0.93	1.13	1.28	2.17	3.67	6.72
CaO	10.77	9.28	11.51	11.42	8.94	4.27	1.95
Na_2O	1.45	1.91	1.08	1.12	1.51	0.16	0.09
K_2O	1.87	1.98	1.89	1.89	1.86	0.24	0
P_2O_5	0	0	0.17	0.06	0	0.08	0
Total	94.65	96.35	100.26	99.75	99.32	99.66	100.14
Number of ions on the basis of 23 oxygens;							6 oxygens:
Si	6.515	6.169	6.103	6.232	6.461	1.949	1.960
Al(IV)	1.485	1.831	1.879	1.768	1.539	0.051	0
Al(VI)	0.374	0.868	0.301	0.663	0.290	0.027	0
Ti	0.068	0.038	0.145	0.122	0.187	0.029	0.011
Fe	4.476	4.099	4.468	4.010	4.398	1.457	1.520
Mn	0.023	0.068	0.067	0.017	0.080	0.030	0.027
Mg	0.149	0.271	0.302	0.519	0.230	0.419	
Ca	1.957	1.631	1.983	1.934	1.537	0.192	0.087
Na	0.477	0.607	0.337	0.343	0.440	0.013	0.007
K	0.405	0.414	0.388	0.381	0.381	0.013	0
P	0	0	0.023	0.008	0	0.003	0
O	23.000	23.000	23.000	23.000	23.000	6.000	6.000
mg	3.2	5.2	5.6	7.0	10.4	13.4	21.3
Mg						12.2	20.7
Fe						77.5	75.0
Ca						10.2	4.3

* total iron as FeO, mg = 100 Mg/(Mg + Mn + Fe)

1) Ferroedenitic hornblende, dyke No. 31, Vallkulla, Sibbo kyrkoby
2) Ferropargasite, ,, ,, 12, Östersundom
3) Hastingsite, ,, ,, 32, Vallkulla, Sibbo kyrkoby
4) Ferropargasite, ,, ,, 40, Road and railway cutting on the Nickby-Sköldvik road, parish of Borgå.
5) Hastingsitic hornblende, ,, 9, Ringberga
6) Pigeonite, ,, ,, 11, specimen A, Östersundom
7) Orthoferrosilite, ,, ,, 11, ,, B,

given in Table 10. Calculated on the basis of 23 oxygens, they thus eliminate the influence of H_2O, F and Cl. The 100 Mg / (Mg + Fe + Mn) varies from ~3 to ~10 in the samples analysed (see Table 10). Table 10 reveals that the hornblende constitutes a series ranging from ferroedenitic hornblende to hastingsite or ferropargasite, depending on the iron-aluminium contents. Ferropargasite holds Al in six-fold co-ordination, whereas hastingsite holds Fe^{3+}. Microprobe does not permit a distinction to be made between Fe^{2+} and Fe^{3+}, but the high Al(VI) and the low Fe together with low Si in analyses 2 and 4 in Table 10 indicate ferropargasite.

Pyroxene was only encountered in dykes 11 and 18. The pyroxene varieties are extremely rich in iron and occurs only as sparse phenocrysts. The analyses (Table 10) indicate that the pyroxenes are near ferrosilite in composition (Pigeonite and orthoferrosilite).

Olivine is only encountered in the same

dykes as pyroxene, and then as almost completely altered grains. Using energy dispersive spectrometry, however, it was possible to find out qualitatively that the olivine in the very small remnants was a fayalite.

AGE OF THE DYKES

Radiometric ages have been reported from all the rapakivi massifs and from the small granite bodies, Onas, Bodom and Obbnäs, in southern Finland. Vaasjoki (1977) reports 1645 Ma as the best age estimate for these small granite bodies, and he concludes that they are definitely younger than the bulk of the Wiborg massif and very likely contemporaneous with the Ahvenisto massif.

According to Vaasjoki (*op.cit.*), the oldest Finnish rapakivi granites belong to the Wiborg massif (1700—1640 Ma), which is divided into three main magmatic phases: 1700—1660 Ma including the Suomenniemi satellite and the porphyries of Hogland; 1660—1640 Ma including the Ahvenisto satellite massif; and 1640 ± 15 Ma in the Kymi cupola. The main phases of the Åland massif are 1670—1620 Ma; the Vehmaa massif is 1590—1530 Ma; the Laitila massif 1570 Ma; and the Ytö granite 1540 Ma.

The isotope zircon age of the Sibbo dykes was determined (branch of isotope geology at Geological Survey of Finland) on dyke No. 11 at Östersundom. The model age calculated was 1633 Ma. The U-Pb concordia diagram for

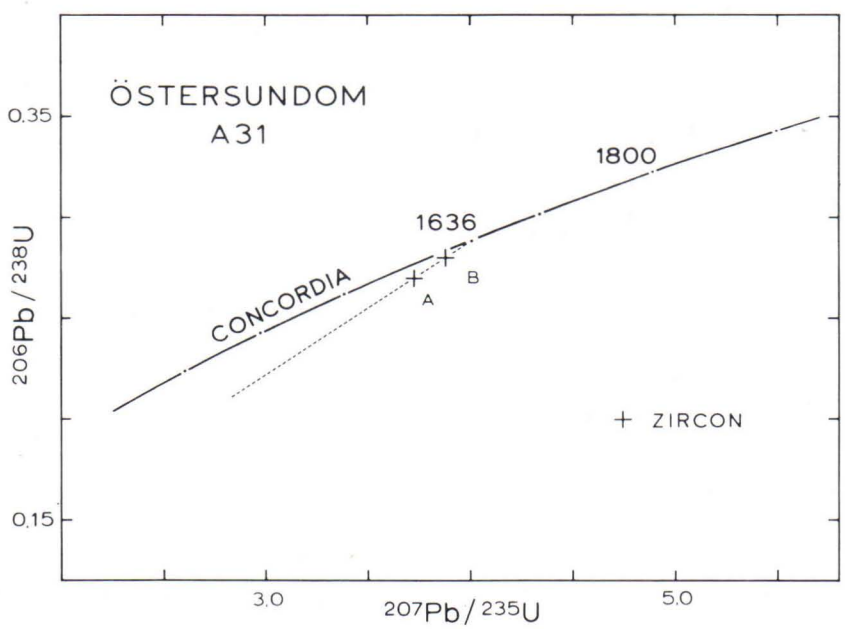

Fig. 20. U-Pb concordia diagram for zircons from dyke No. 11 at Östersundom (sample A 31). The dashed line indicates a continuous diffusion trajectory (Wasserburg 1963) for a primary age of 1636 Ma. The corresponding chords for single points would be 1639 Ma (A) and 1633 Ma (B).

Table 11. U—Pb analytical data for zircons from dyke No 11, Östersundom.

Sample No.	Zircon fraction $d = g/cm^3$ HF = preleached in HF	^{238}U ppm	Radiogenic ^{206}Pb, ppm	$\frac{^{206}Pb}{^{204}Pb}$ measured	Isotopic abundance relative to ^{206}Pb (= 100)			Radiometric ages, Ma		
					204	207	208	$\frac{^{206}Pb}{^{238}U}$	$\frac{^{207}Pb}{^{235}U}$	$\frac{^{207}Pb}{^{206}Pb}$
A31A	d>4.6	95.13	22.18	1771	0.053479	10.771	31.915	1538 ± 8	1577 ± 5	1630 ± 7
B	d>4.6; HF	81.21	19.70	2264	0.040094	10.593	29.269	1593 ± 8	1609 ± 5	1631 ± 6

zircon is given in Fig. 20 and the U-Pb analytical data in Table 11. Recalculated data from the Onas granite give almost the same model age 1630 ± 10 Ma (Laitala 1984).

The isotopic data available indicate clearly the genetic connection between the dykes of Sibbo and the Onas granite.

PETROGENESIS

The genetic connection between the dykes and the Onas granite, suggested by several authors (Borgström 1907, 1947, Vorma 1976, Härme 1978), has now also been proved by radiometric age determinations. Accordingly, the dykes of Sibbo and the Onas granite are from the same magmatic period (1630 ± 15 Ma), that is, considerably younger than the surrounding early Middle Proterozoic migmatites, microcline granites and gneisses (1800 Ma).

Contrary to earlier suggestions that the granite porphyry dykes of Sibbo were apophyses of the Onas granite, the present author proposes that the dykes were emplaced before the intrusion of the Onas granite. Several factors support this: 1) porphyry dykes have not been encountered within the Onas granite, 2) the Onas granite is more differentiated than the dykes, as has been shown petrochemically: a) the more basic character of the dykes (DI in Table 3), b) the high Ti content, c) the ZrO_2/TiO_2 and ZrO_2/SiO_2 correlations (Fig. 14), d) the REE distribution (Table 6 and Fig. 15).

The chemical composition of the Sibbo dykes is normal granitic, but most of the dykes have a rather low, and some a very low, SiO_2 content and a rather high TiO_2, FeO (Fe_2O_3) and CaO content. In many respects these dykes closely resemble the granite porphyry of group 5a from Schwarzwald, described by Schleicher (1978).

It may be inferred from the intimate association of the dykes in space and from their chemical composition that a magma or a series of magmas with a close genetic relation to one another and to the Onas granite, and which were most certainly derived from a common parent, intruded as a dyke swarm in Sibbo.

The form and occurrence of the dykes suggest that they may have been intruded into an extension field. A common consequence of shear zone displacement under brittle-ductile conditions is the development of extension fractures oriented at angles of about 30°—45° to the trend of the shear zone (Cloos 1955, Ramsay 1980).

The main fold axis in the southern part of the Svecofennides in southern Finland, trends

ENE. A fracture system trending NW—NNW was generated as a consequence of compressions working in a SSE—NNW direction during the Svecokarelidic orogeny in Middle Proterozoic time (Talvitie 1979).

The author now suggests that extensional fractures trending NW—SE were generated in a brittle-ductile crust as a result of shearing during the Svecokarelidic orogeny. The fractures were subsequently reactivated and enlarged and, in accordance with the discussion above by Cloos (*op.cit.*) and Ramsay (*op.cit.*), a sinistral en echelon fracture system formed because of E—W compression during the extensive late Middle Proterozoic rapakivi magma activities and was occupied by dykes.

Apophyses and some offsets of the horn type, from some millimetres to about 10 cm wide, are frequently encountered among the Sibbo dykes. Currie and Ferguson (1970) discuss the likelihood of magma penetrating a fissure; *i.e.* how long and how wide a fissure must or can be, taking into account the temperature, density and viscosity of the magma and the pressure head that pushes the magma along the fissure. They conclude that small offsets (~ 1 cm) would hardly ever be intruded. To explain the occurrence of such apophyses and offsets they propose an intrusion mechanism characteristic of volatile and gas-rich magmas.

When a magma comes into contact with an opening fissure, the pressure must drop drastically. If the magma is initially saturated with volatiles they would boil off, and the volatile phase would rush into the fissure and penetrate the apophyses. This would result in the formation of a thin layer of chilled silicate material along the margins or possibly of a material of different composition, depending on the constituents of the volatiles (Currie & Ferguson, *op.cit.*).

The observations from Sibbo, however, suggest a somewhat different intrusion mechanism for the porphyries. There are no essential differences in composition between the contacts and the central parts of the dykes, and no contact interaction has been seen in the host rock. Therefore, the temperature of the magma had already fallen considerably at the time of intrusion. The occurrence of primary biotite and amphibole indicates a hydrous magma. The apophyses may have been formed as described by Currie and Ferguson (*op.cit.*) even though the fissures were filled with a liquid water-rich magma of the same composition as the main porphyry rather than a gas phase.

From the presence of the chilled dyke margins, it is evident that the host was considerably lower in temperature than the solidus of the dyke magma at the time of intrusion. The dykes must have cooled rapidly to form the fine-grained minerals and the aphanitic contact zone in the hypersolidus temperature range and then cooled more slowly to form the subsolidus minerals through devitrification, partly at temperatures higher than that of the host rock.

The presence of porphyritic contact zones with the same phenocrysts as in the inner part of the dyke shows that the intruded magma already contained some phenocrysts at least. The data from the two-felspar geothermometer also support this: the groundmass solidified at a temperature $<400°C$ and the phenocrysts probably at 530°—700°C. Thus the groundmass solidified from a considerably undercooled magma.

It must be emphasised that the temperature measured in the matrix is not necessarily that of matrix crystallisation, but one that lasted for such a long time that equilibrium was reached, at least in parts of the rock, and so some recrystallisation could occur.

Some of the phenocrysts show resorption and in places they are severely corroded. Cavities in the phenocrysts are filled with matrix material. Corrosion is often seen around the quartz grains in the phenocrysts of intergrown K-felspar and quartz (Fig. 21). The

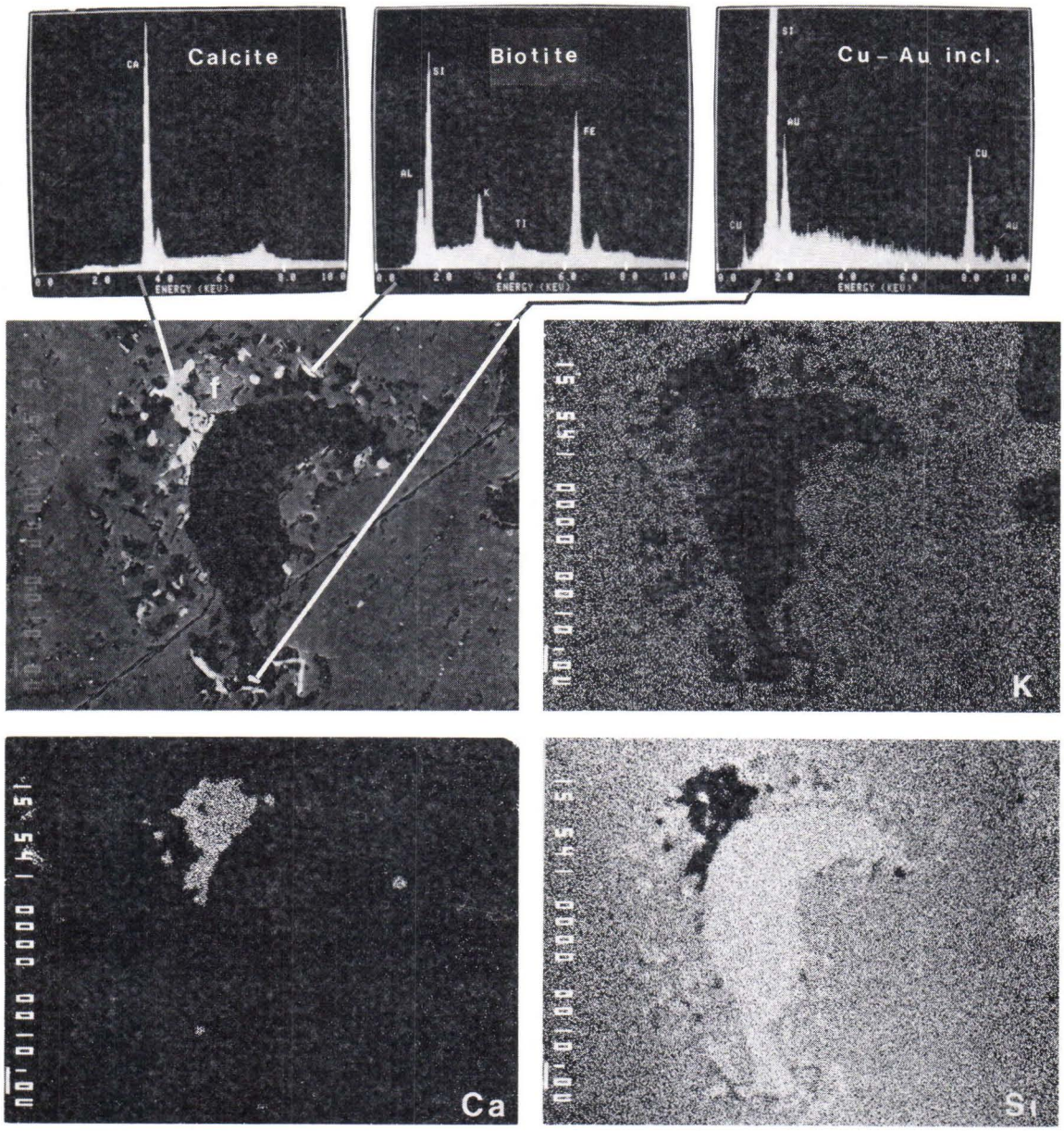

Fig. 21. Backscattered electron image of a corroded part around a quartz grain in the phenocryst with intergrown K-felspar and quartz shown in Fig. 5, and X-ray distribution patterns for K, Ca and Si. The three EDS spectra show examples of secondary mineral "inclusions". f = fluorite, length of bar = 10 μm.

occurrence of secondary fluorite, calcite and metals is seen from the X-ray distribution patterns. It is inferred that the corroding medium was a fluorine rich liquid, which also carried some metals, as indicated by the existence of native Cu and Au (Fig. 21).

Less calcic plagioclase phenocrysts may have crystallised at a very late stage of cooling or they may also be products of devitrification due to slow cooling of the dykes at the last stage of the cooling history. Clear devitrification products (spherulites, crystallites) occur in some dykes and in the chilled margins.

The porphyry dykes are some of the youngest rocks in the area, 1633 Ma as against 1800 Ma for the country rocks. Since their emplacement, the only other process that could have caused alterations in the dykes was the final stages of rapakivi magma activity in southern Finland.

But, as stated, alterations occur in the dykes. Some of the alteration reactions occurred only within phenocrysts and are hence inferred to belong to the intratelluric stage of the crystallisation history. Alteration of this type is seen in the ilmenomagnetite—titanite assemblages. On the other hand, where magnetite or ilmenomagnetite are in contact with orthoclase or plagioclase, they reacted, forming amphibole (ferrohastingsite), biotite, calcite, quartz and titanite. In some places the oxides have been totally replaced, and only a skeleton structure (pseudomorph) built up of amphibole and biotite reflects the contours of the old crystal. Later alterations are chloritisation of biotite and chloritisation and sericitisation of plagioclase (in some instances total alterations).

Because the biotite and amphibole often form a corona around the Ti-mineral phenocrysts, the matrix liquid is presumed to have reacted with the phenocrysts and probably also to have supplied some of the calcium required for building up the titanite and amphibole. This may have been possible during the emplacement of the dykes when the P and T conditions were abruptly changed.

The present author proposes heat flow from the rapakivi magma and pore fluids related to the crystallisation of the Onas granite as the most common reason for the alterations that took place after the emplacement of the dykes or the matrix condensation.

It is an interesting fact that in the phenocrysts studied by the author the K-felspar phenocrysts without quartz inclusions have a smoothly increasing Ba distribution from core to margin. These phenocrysts often show an especially steep jump in the Ba content at the rim (see Fig. 17). These phenomena are obviously due to a Ba-rich pulse at a stage of the crystallisation history when only some phenocrysts were developed and Ba was diffused into these crystals. The lack of barium in the matrix shows clearly that this Ba pulse occurred before the intrusion. Also the lack of Ba in the phenocrysts of intergrown K-felspar and quartz indicates that they crystallised at a very late stage or at a time of intrusion when the pressure was drastically lowered and the magma was water saturated (see below), in any case after the Ba pulse.

Thus, as stated by Mehnert and Büsch (1981), there is no reason to determine the Ba values in a phenocryst as a whole; only comprehensive study of the Ba distribution within a crystal gives useful results.

In accordance with the investigations by Mehnert and Büsch (*op.cit.* p. 237—241) (see also discussion on p. 9), at least in some cases rather small, rounded single crystals of K-felspar and quartz grew together at the early stages to form phenocrysts. Some, but not all, of the intergrowths of quartz and K-felspar may have developed in that way (Fig. 22).

The formation of granophyre in the groundmass may be explained by the presence of a hydrous vapour phase during the late stages of the crystallisation history. Elliot (1977) shows that simultaneous crystallisation of two min-

Fig. 22. Photomicrograph of a quartz-felspar crystal aggregate of several single quartz and felspar grains. Dyke No. 4, polished thin section, 2.5 X.

erals may be coupled or uncoupled. If one phase grows into the melt in advance of the other, which fills the space left, the two phases form independently of one another and growth is said to be uncoupled. Coupled growth implies that the processes involved in the growth of the two minerals are intimately related. The two minerals grew with similar velocities, exceeding that of either of the phases separately. Coupled eutectic growth may occur at any composition below the eutectic temperature and outside the solubility limit of the single phases (Woodruff 1973). According to Carstens (1983), for growth to occur at off-eutectic compositions it is only necessary for the average liquid composition at the solid-liquid interface to be near the eutectic composition. This may occur by solute build-up at the interface. The volume fractions of the constituent phases adjust to the liquid composition. Therefore it is not necessary for quartz and felspar to be present in eutectic (cotectic) proportions for simultaneous growth.

Hunt and Jackson (1966) showed that growth morphology in an eutectic system is essentially determined by faceting behaviour of the individual phases. This is related to the structure of the solid-liquid interface and may be predicted in simple compounds growing from their own melts from the entropy of fusion values.

Quartz and felspar differ markedly in faceting behaviour. Quartz grows with rounded shapes in many rhyolites containing quartz and sanidine phenocrysts in contrast to felspar, which always has faceted interfaces and grows by a layer-spreading mechanism. This is consistent with their entropy of fusion values (Carmichael *et al.* 1974). Quartz, however, is often faceted when grown from a melt rich in water and at large degrees of undercooling, and the growth of a felspar crystal may be nonfaceted because of roughening of the faces (Dowty 1980). The faceting tendency appears to vary with the composition and undercooling of the melt.

Carstens (1983) concludes that a spherulitic structure forms from a coupled nonfaceted growth of both felspar and quartz; an hourglass structure by coupled growth of faceted felspar and nonfaceted quartz; cuneiform granophyric intergrowths from a noncoupled faceted-faceted growth; and other structures from a noncoupled faceted-nonfaceted growth mechanism.

Granophyric and spherulitic structures may occur in the same thin section. This indicates a growth mechanism highly sensitive to changes in the solidification conditions. Hourglass and spherulitic structures often grade into a granophyric structure. A transition from coupled to noncoupled growth appears to take place during solidification. This may be related to a change in the growth mechanism, *i.e.* to a change from nonfaceted to faceted growth for one or both of the minerals. Elwell and Scheel (1975) have shown that adsorption of impurity elements may change the growth mechanism.

Water, which is insoluble in both phases, may be a considerable factor. During freezing

it will become concentrated adjacent to the solid-liquid interface. This diluted melt may be responsible for a change in the faceting behaviour towards a greater tendency to facet and hence from coupled to uncoupled growth (Carstens 1983).

During crystallisation the H_2O content of the residual magma increases, and faceting behaviour such as that described above caused by a hydrous magma is proposed as the reason for the well-developed, beautiful granophyric structures seen in the inner parts of the Sibbo dykes. As mentioned the spherulites in these dykes were formerly considered to have developed through devitrification.

Amygdales, which are frequently encountered in the dykes, are filled with secondary minerals, calcite, quartz, chlorite, fluorite and biotite. According to Peck (1978), the formation of vesicles is limited to the upper part of a cooling magma. It has therefore been proposed that the occurrence of amygdales should indicate that the upper parts of the dykes are exposed. There may be another explanation however. As discussed above, when a fracture is opening, the pressure drops drastically and the magma boils. The intruding magma should therefore be expected to "carry" vesicles throughout the dyke, not only in the shallow parts.

Some of the dykes show interaction with the country rock (Nos. 3, 28, 40 and 53). Chilled margins are not seen clearly. Under the microscope the contact is not sharp, small pieces of country rock having been assimilated into the dyke, and the dyke may show slight brecciation. Near the border the groundmass shows beautiful flow structures. The phenocrysts are cataclastically broken, and quartz is rolled out and to some extent recrystallised. These dykes are inferred to be syntectonic, having intruded at the same time as the wall rock underwent shearing.

SUMMARY

Contrary to earlier suggestions that the granite porphyry dykes of Sibbo are apophyses of the Onas granite, the present author proposes that the dykes were emplaced before the intrusion of the Onas granite.

The Sibbo dykes were emplaced into early Middle Proterozoic rocks in the southern Svecofennides. They occupy a northwest-trending fracture system that in places is discordant to, and in places concordant with, the Proterozoic tectonic directions in the area.

Radiometric age determinations and the general petrological and mineralogical character of the dykes indicate a close genetic connection with the rapakivi granites, especially the Onas granite. The dyke suite shows a slight differentiation within a SiO_2 range of 59 wt % to 72 wt %, ending in the composition of the Onas granite. Radiometric age determination performed using the uranium-lead method indicates an age of 1633 Ma for the dykes, or about the same as that determined previously for the Onas granite (1630 ± 10 Ma).

The major constituents of the dykes are monoclinic K-felspar, orthoclase, partly altered plagioclase (An_0 - An_{70}), quartz, biotite and hornblende (ferropargasite, ferroedenite and hastingsite). In some instances the biotite and plagioclase are partly chloritised. Accessories are apatite, zircon, ilmenomagnetite, fluorite, calcite and rare sulphides. In two dykes sparse phenocrysts of pyroxene and fayalite are encountered. Granophyric intergrowths are very common and present in almost all the dykes. They are inferred to have been formed by the interaction of a hydrous phase during the final

stages of matrix crystallisation. The two-feldspar geothermometer gives model felspar equilibrium temperatures of $<1400°C$ for the matrix, and a range of 530°C to 700°C for the phenocrysts.

The occurrence of amygdales, primary amphibole and biotite and the low thermal state of the K-felspar suggest that the magma was water saturated. Late-stage activity of volatiles is verified by various alteration phenomena (serisitisation, chloritisation, corrosion and native metal deposition). These secondary reactions were obviously caused by heat flow from the rapakivi magma and related pore fluids generated during the crystallisation of the Onas granite.

ACKNOWLEDGEMENTS

The author expresses his gratitude to Dr. Olavi Kouvo (Geological Survey of Finland) for arranging the radiometric age determinations; to Mr. Väinö Hoffrén, (Geol. Surv.) for the XRF analyses; to Miss Maija Kaistila, (Reactor Laboratory, Technical Research Centre of Finland) for the neutron activation analyses; to Professor Ilmari Haapala (University of Helsingfors), Dr. Kai Hytönen and Dr. Kari Kinnunen (Geol. Surv.) for their helpful reviews of the manuscript; to Professor. Jouko Talvitie (Geol. Surv.) for valuable discussions; to Dr. Matti Laitala (Geol. Surv.) for providing specimen 107/La/60 from Fårholmen; to Miss Taina Koivisto and Miss Sari Lehtola (Geol. Surv.) for drawing the figures; to Mr. Bo Johanson and Mrs. Mirja Saarinen (Geol. Surv.) for assistance in the laboratory; and to Mrs. Gillian Häkli for correcting the English.

REFERENCES

Anfilogov, V. N., Glyuk, D. S. & Trufanova, L. G., 1973. Phase relations in interaction between granite and sodium fluoride at water vapor pressure of 1000 kg/cm. Geochem. Int. 10, 30—33.

Augustithis, S. S., 1973. Atlas of textural patterns of granites, gneisses and associated rock types. Elsevier Scientific Publ., Amsterdam, 378 p.

Barker, D. S., 1970. Compositions of granophyre, myrmekite and graphic granite. Geol. Soc. Amer., Bull. 81, 3339—3350.

Borgström, L. H., 1907. Granitporphyr von Östersundom. Bull. Comm. géol. Finlande 22, 20 p.

—, **1931.** Das Granitgebiet von Onas. Centraltryckeriet,Helsingfors, 7 p.

— ,**1947.** Granite-porphyry from Östersundom II. Bull. Comm. géol. Finlande 140, 121—128.

Bowden, P. & Whitley, J. E., 1974. Rare earth patterns in peralkaline and associated granites. Lithos 7, 15—21.

Carmichael, J. S. E., Turner, F. J. & Verhoogen, J., 1974. Igneous petrology. McGraw-Hill, New York, 739 p.

Carstens, H., 1983. Simultaneous crystallisation of quartz-feldspar intergrowths from granitic magmas. Geology 11, 339—341.

Cloos, E., 1955. Experimental analysis of fracture patterns. Geol. Soc. America, Bull. 66, 241—256.

Currie, K. L. & Ferguson, J., 1970. The mechanism of intrusion of lamprophyre dikes indicated by "offsettings" of dikes. Tectonophysics 9, 525—535.

Dowty, E., 1980. Crystal growth and nucleation theory and numerical simulation of igneous crystallisation. *In* Physics of magmatic processes, ed. by R.B. Hargraves, 419—485, Princeton University Press, Princeton, New Jersey.

Drescher-Kaden, F. K., 1948. Die Feldspat-Quarz-Reaktionsgefüge der Granite und Gneise und ihre genetische Bedeutung. Springer Verlag, Berlin—Göttingen—Heidelberg, 259 p.

—, **1969.** Granitprobleme. Akademie Verlag, Berlin, 586 p.

—, **1974.** Aplitische Gänge in Graniten und Gneisen. Walter de Gruyter, Berlin—New York, 215 p.

Elliot, R., 1977. Eutectic solidification. Intern. Metals Rev. 22, 161—186.

Elwell, D. & Scheel, H. J., 1975. Crystal growth from high—temperature solutions. Academic Press, London, 634 p.

Eskola, P., 1934. Über die Bottenmeerporphyre. Bull. Comm. géol. Finlande 104, 111—127.

Emmermann, R., Daieva, L. & Schneider, J., 1975. Petrologic significance of rare earth distribution in granites. Contr. Mineral. Petrol. 52, 267—283.

Goldsmith, J. R. & Laves, F., 1954. The microcline—sanidine stability relations. Geoch. Cosmoch. Acta 5, 1—19.

Guidotti, C. V., Herd, H. H. & Tuttle, C. L., 1973. Composition and structural state of K-feldspars from K-feldspar + sillimanite grade rocks in northwestern Maine. Amer. Mineral. 58, 705—716.

Haapala, I., 1977. Petrography and geochemistry of the Eurajoki stock, a rapakivi-granite complex with greisen-type mineralization in southwestern Finland. Geol. Surv. Finland, Bull. 286, 128 p.

Hackman, V., 1905. Die chemische Beschaffenheit von Eruptivgesteinen Finnlands und der Halbinsel Kola in Lichte des neuen amerikanischen Systemes. Bull. Comm. géol. Finlande 15, 143 p.

Härme, M., 1978. Geological map of Finland 1:100 000, sheets 2043—2044 Kerava—Riihimäki. Explanation to the maps of rocks. Geol. Surv. Finland, 51 p.

Herrmann, A. G., 1970. Yttrium and lanthanides. *In* Handbook of Geochemistry, ed. by K.H. Wedepohl, Springer Verlag, Berlin—Heidelberg—New York.

Homma, F., 1936. Classification of the zonal structure of plagioclase. Mem. College Sci. Kyoto Imp. Univ., Ser. B 11, 135—155.

Hunt, J. D. & Jackson, K. A., 1966. Binary eutectic solidification. Amer. Inst. Mining Eng., Metallurg. Soc. Transact. 236, 843—852.

Irvine, T. N. & Baragar, W. R. A., 1971. A guide to the chemical classification of the common volcanic rocks. Canad. J. Earth Sci. 8, 523—548.

James, R. S. & Hamilton, D. L., 1969. Phase relations in the system $NaAlSi_3O_8$ - $KAlSi_3O_8$ - $CaAl_2Si_2O_8$ - SiO_2 at 1 kilobar water vapor pressure. Contr. Mineral. Petrol. 21, 111—141.

Kovalenko, V. I. 1973. Distribution of fluorine in a topaz-bearing quartz keratophyre dike (ongonite) and solubility of fluorine in granitic melts. Geochem. Int. 10, 41—49.

Kovalenko, V. I., Kuzmin, M. I., Antipin, V. S. & Petrov, L. L., 1971. Topaz-bearing quartz keratophyre (ongonite), a new variety of subvolcanic igneous vein

rock. Dokl. Akad. Nauk USSR, Earth Sci. Sect. 199, 132—135.

Laitala, M., 1984. Geological map of Finland 1:100 000, sheets 3012 and 3021 Pellinge—Porvoo. Explanation to the maps of rocks. Geol. Surv. Finland, 53 p.

de La Roche, H, le Terrier, P., Grandclaude, P. & Marchal, M., 1980. A classification of volcanic and plutonic rocks using R_1R_2-diagram and major-element analyses. Its relationship with current nomenclature. Chem. Geol. 29, 183—210.

Le Maitre, R. W., 1976. The chemical variability of some common igneous rocks. Journ. Petrol. 17, 589—637.

Lemberg, J., 1867. Die Gebirgsarten der Insel Hochland, chemisch geognostisch untersucht. Archiv für Naturkunde Liv-, Est- und Kurlands, 1. Serie Bd. 4, Dorpat, 174—222.

Manning, D. A. C., Hamilton, D. L., Henderson, C. M. B. & Dempsey, M. J., 1980. The probable occurrence of interstitial Al in hydrous, F-bearing and F-free aluminosilicate melts. Contr. Mineral. Petrol. 75, 257—262

Mehnert, K. R. & Büsch, W., 1981. The Ba content of K-feldspar megacrysts in granites: a criterion for their formation. N. Jb. Mineral. Abh. 140, 221—252.

Middlemost, E. A. K., 1972. A simple classification of volcanic rocks. Bull. Volcanol. 24, 383—397.

Murthy, M. V. N., 1958. On the crystallization of accessory zircon in granitic rocks of magmatic origin. Canad. Mineral. 6, 260—263.

Nieminen, K. & Yliruokanen, I,. 1974. Trace element analysis of granitic and radioactive rocks by spark source spectrometry with electrical detection. Bull. Geol. Soc. Finland 46, 167—176.

Nockolds, S. R., 1947. The relation between chemical composition and paragenesis in the biotite mica of igneous rocks. Amer. Journ. Sci. 245, 401—420.

—, **1954.** Average chemical compositions of some igneous rocks. Geol. Soc. America, Bull. 65, 1007—1032.

Peck, D. L., 1978. Cooling and vesiculation of Alae Lava Lake, Hawaii. U.S. Geol. Surv. prof. paper 935-B, 59 p.

Pehrman, G., 1941. En gång av kvartsporfyr på Runsala holme invid Åbo. Geol. fören. Stockh. förh. 63, 426, 197—202.

von Platen, H., 1965. Kristallisation granitischer Schmelzen. Contr. Mineral. Petrol. 11, 334—381.

Poldervaart, A., 1956. Zircon in rocks. 2. Igneous rocks. Amer. J. Sci. 254, 521—554.

Ramsay, J. G., 1980. Shear zone geometry: a review. Journ. Struct. Geol. 2, 83—99.

Riederer, J., 1965. Die Kalifeldspäte der moldanubischen Granite. N. Jb. Mineral. Abh. 102, 291—339.

Roedder, E., 1972. Composition of fluid inclusions. U.S. Geol. Surv. prof. paper 440—JJ, 164 p.

Rosenbusch, H. - Osann, A., 1923. Elemente der Gesteinslehre. E. Schweizerbart'sche Verlagsbuchhandlung (E. Nägele) Stuttgart, 779 p.

Saastamoinen, J., 1956. Graniittiporfyyri- ja breksiajuonista Etelä-Sipoossa. Unpubl. thesis. Archives of the Dept. of Geology, University of Helsinki, 54 p.

Sahama, Th. G. 1945. On the chemistry of the East fennoscandian rapakivi granites. Bull. Comm. géol. Finlande 136, 15—67.

Savolahti, A., 1956. The Ahvenisto massif in Finland. Bull. Comm. géol. Finlande 174, 96 p.

Schleicher, H., 1978. Petrologie der Granitporphyre des Schwarzwaldes. N. Jb. Mineral. Abh. 132, 153—181.

Sederholm, J. J., 1934. On migmatites and associated pre-Cambrian rocks of southwestern Finland. Part III, The Åland island. Bull. Comm. géol. Finlande 107, 68 p.

Simonen, A. & Vorma, A., 1969. Amphibole and biotite from rapakivi. Bull. Comm. géol. Finlande 238, 28 p.

Smith, J. F., 1974. Feldspar minerals 2. Chemical and textural properties. Springer Verlag, Berlin—Heidelberg—New York, 690 p.

Stewart, D. B. & Wright, T. L., 1974. Al/Si order and symmetry of natural alkali feldspars, and the relation of strained cell parameters to bulk composition. Bull. Soc. fr. Minéral. Cristallogr. 97, 356—377.

Stormer, J. C., 1975. A practical two-feldspar geothermometer. Amer. Mineral. 60, 667—674.

Streckeisen, A. & Le Maitre, R. W., 1979. A chemical approximation to the model QAPF classification of the igneous rocks. N. Jb. Mineral. Abh. 136, 169—206

Talvitie, J., 1979. Seismo-tectonics in Finland. Geol. Fören. Stockh. Förhandl. 100, 247—253.

Thornton, C. P. & Tuttle, O. F., 1960. Chemistry of igneous rocks, I. Differentiation index. Amer. J. Sci. 258, 664—684.

Tuttle, O.F. & Bowen, N.L., 1958. Origin of granite in the light of experimental studies in the system $NaAlSi_3O_8$ - $KAlSi_3O_8$ - SiO_2- H_2O. Geol. Soc. America Mem. 74, 153 p.

Vaasjoki, M., 1977. Rapakivi granites and other postorogenic rocks in Finland: their age and lead isotopic composition of certain associated galena mineralizations. Geol. Surv. Finland, Bull. 294, 64 p.

Vlasov, K. A., (editor) 1968. Geochemistry and mineralogy of rare elements and genetic types of their deposits. III. Genetic types of rare element deposits. Acad. Sci. USSR. Ministr.Geol. USSR. Israel Program for Scientific Translations, Jerusalem, 916 p.

Vorma, A., 1971. Alkali feldspars of the Wiborg rapakivi massif in southeastern Finland. Bull. Comm. géol. Finlande 246, 72 p.

—, **1975.** On two roof pendants in the Wiborg rapakivi massif, soutwestern Finland. Geol. Surv. Finland, Bull. 272, 86 p.

—, **1976.** On the petrochemistry of rapakivi granites with

—, **1976.** On the petrochemistry of rapakivi granites with special reference to the Laitila massif, southwestern Finland. Geol. Surv. Finland, Bull. 285, 98 p.

Wahl, W., 1947. A composite lava flow from Lounatkorkia, Hogland. Bull. Comm. géol. Finlande 140, 287—302.

Wasserburg, G. J., 1963. Diffusion processes in lead-uranium systems. J. Geophys. Res. 68, 4823—4846.

Whitney, J. A. & Stormer, J. C., 1976. Geothermometry and geobarometry in epizonal granitic intrusions: a comparison of irontitanium oxides and coexisting feldspars. Amer. Mineral. 61, 751—761.

—, **1977.** Two-feldspar geothermonetry, geobarometry in mesozonal granitic intrusions: Three examples from the Piedmont of Georgia. Contr. Mineral. Petrol. 63, 51—64.

Winkler, H. F. G., 1974. Petrogenesis of metamorphic rocks. 3rd edit. Springer-Verlag, Berlin—Heidelberg—New York 320 p.

Winkler, H. F. G. & Breitbart, R., 1978. New aspects of granitic magmas. N. Jb. Mineral. Mh. H. 10, 463—480.

Winkler, H. F. G. & Schultes, H., 1982. On the problem of alkali feldspar phenocrysts in granitic rocks. N. Jb. Mineral. Mh. H. 12, 558—564.

Woodruff, D. R., 1973. The solid-liquid interface. University Press, London—Cambridge, 182 p.

Wright, T. L., 1967. The microcline—orthoclase transformation in the contact aureole of the El-dora stock, Colorado. Amer. Mineral. 52, 117—136.

ERRATA

p. 6, right col., line 1 — **for** author the **read** author in the

p. 10, right col., line 8 — **for** (orthoferrosilite) (analysis **read** (orthoferrosilite) and pigeonite (analysis

p. 27, expl. to Table 7c, line 2 — **for** 4) **read** 4).

p. 28 right col., line 3 — **for** $d_{\overline{131}}$ **read** $d_{1\bar{3}1}$

p. 28 right col., line 5 — **for** $d_{\overline{131}}$ **read** $d_{1\bar{3}1}$

p. 28 expl. to Fig 18, line 1 — **for** $d_{\overline{204}}$ **read** $d_{\bar{2}04}$

p. 29 text to Table 8, line 3 — **for** $d_{\overline{131}}$ **read** $d_{1\bar{3}1}$

p. 32 right col. 2nd line from bottom — **for** (Pigeonite **read** (pigeonite

p. 40 left col., line 3 — **for** $<1400°C$ **read** $<400°C$

p. 15, Table 3.

Table 3. Selected microprobe analyses of the Sibbo dyke rocks (wt. %).

	1	2	3	4	5	6	7	8	9	10	11	12
. . . . .												
correct lines to												
il	1.80	1.41		1.12	0.68	0.40	1.31	0.08	0.99	0.72	0.86	0.32
ap	0.31	0.55		0.47	0.57	0.10	0.50	0.19			0.24	0.12
. . . . .												

p. 27, Table 7c.

Table 7c. Selected microprobe analyses of chemically zoned felspar phenocrysts from the dykes of Sibbo (wt. %).

	1	2	3	4	5	6
. . . . .						
correct line to						
Mn	0	0	0	0	0	0.004
. . . . .						

Tata julkaisua myy

VALTION PAINATUSKESKUS

POSTIMYYNTI

PL 516
00101 Helsinki 10
Vaihde (90) 539 011

KIRJAKAUPAT HELSINGISSÄ

Annankatu 44
(Et. Rautatiekadun kulma)
Vaihde (90) 17 341

Eteläesplanadi 4
Puh. (90) 662 801

Denna publikation säljes av

STATENS TRYCKERICENTRAL

POSTFÖRSÄLJNING

PB 516
00101 Helsingfors 10
Växel (90) 539 011

BOKHANDLAR I HELSINGFORS

Annegatan 44
(i hörnet av S. Järnv.g.)
Växel (90) 17 341

Södra esplanaden 4
Tel. (90) 662 801

This publication can be obtained from

GOVERNMENT PRINTING CENTRE

MAIL-ORDER BUSINESS

P.O.Box 516
SF-00101 Helsinki 10
Phone (90) 539 011

BOOKSHOPS IN HELSINKI

Annankatu 44
Phone (90) 17 341

Eteläesplanadi 4
Phone (90) 662 801

ISBN 951-690-200-6
ISSN 0367-522X